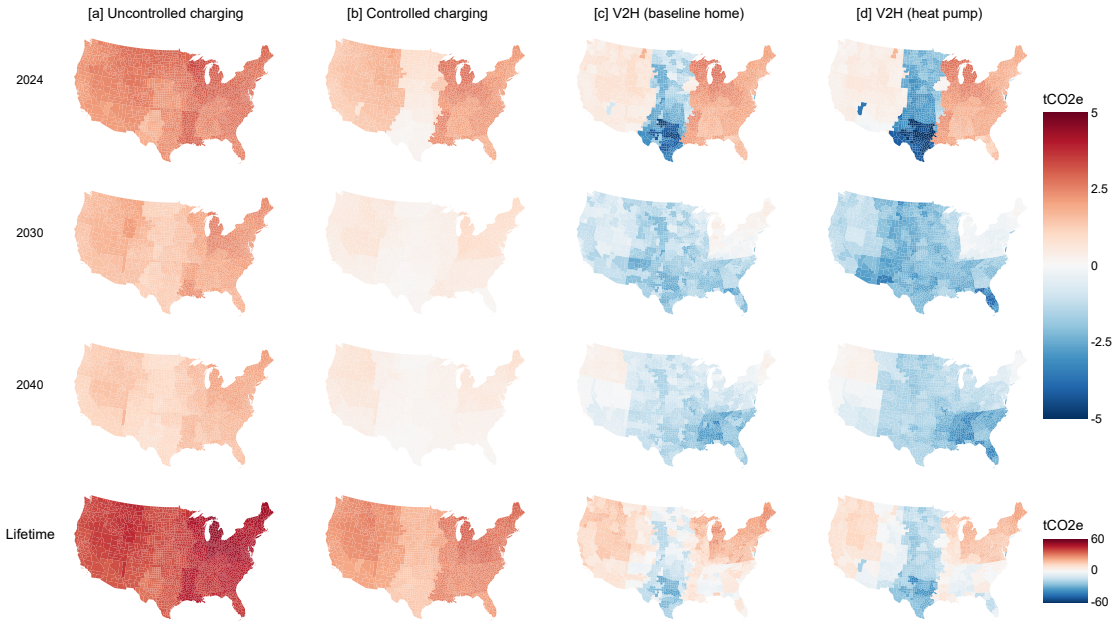


Figure A.20: **Annual charging emissions and life-cycle emissions.** Median annual charging GHG emissions and life-cycle GHG emissions for individual EVs, in each region across the US for **a,** uncontrolled charging; **b,** controlled charging; **c,** V2H for baseline homes; **d,** V2H fully electrified home with heat pump heating. Rows correspond to annual results for 2024, 2030, and 2040, and vehicle-lifetime results. Charging emissions are defined as the net increase in the electricity bill of the whole home after introducing EV charging. Map GeoJSON from Plotly visualization tool[58].

A.3.6 Synergies between whole-home electrification and V2H

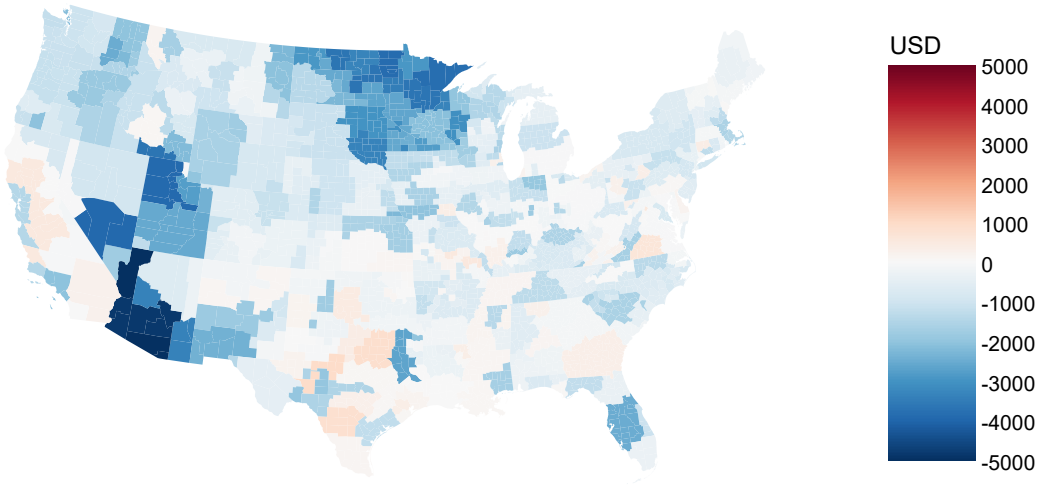


Figure A.21: **Cost synergies between vehicle and whole-home electrification.** Median changes in vehicle lifetime charging costs across the contiguous U.S., switching from V2H (baseline home) to V2H (heat pump). Negative (blue) values indicate synergies; i.e., V2H homes save more than do baseline homes. Map GeoJSON from Plotly visualization tool[58].

The largest synergies are in southern Mountain states and in West North Central states. Synergies in emissions reductions are more widespread than synergies in cost reductions.

A.4 Detailed sensitivity analysis

A.4.1 Charging optimization internalizes social cost of carbon

To test our conclusions' sensitivity to a plausible future in which V2H is optimized to minimize the sum of household electricity costs and GHG externalities, we run our analysis with an objective function including a \$51/t CO_2e GHG externality. In this analysis we do not assume that reductions in monetized GHG externalities are reflected in the customers' bill: there is no carbon tax.

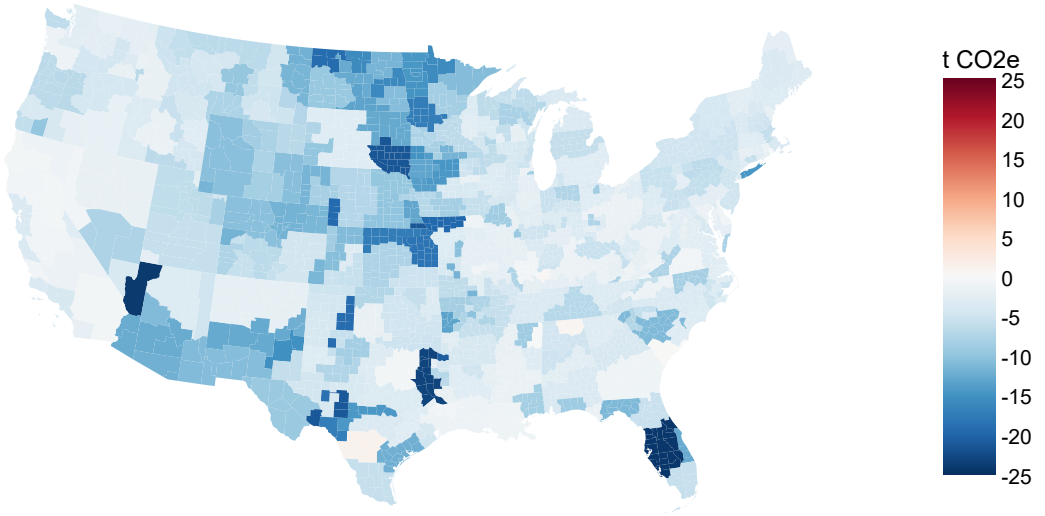


Figure A.22: **Emissions synergies between vehicle and whole-home electrification.** Median changes in vehicle lifetime charging emissions across the contiguous U.S., switching from V2H (baseline home) to V2H (heat pump). Negative (blue) values indicate synergies; i.e., V2H homes reduce emissions more than do baseline homes. Map GeoJSON from Plotly visualization tool[58].

For controlled charging, cost savings are similar whether or not monetized GHG externalities are a part of the objective function. GHG emission reductions from controlled charging are increased by 16–38% relative to a baseline when monetized externalities are accounted for. For V2H in homes with heat pumps, cost savings decrease by 6.0–18% relative to a baseline when monetized GHG externalities are accounted for in deciding when and how much to charge, but the corresponding increase in emission reductions is 70–106%. (see Supplementary Table A.4).

Table A.4. Sensitivity analysis: robustness of results to the assumption of internalized GHG emission externalities.
Cost reductions and GHG emission reductions are estimated compared to the uncontrolled charging baseline, which does not change with this assumption. The numbers in the bracket are the 5th-95th percentile range. V2H (heat pump) means V2H in fully electrified homes. Even when externalities are included in the objective function, they are not reflected in the electricity cost to homeowners

	Average and range of lifetime cost reduction ($1000s)		Average and range of lifetime GHG emission reduction (tCO_2e)	
Obj. function	excl. monetized GHG	incl. monetized GHG	excl. monetized GHG	incl. monetized GHG
Controlled charging	1.72 (1.41–2.00)	1.71 (1.39–2.00)	17.0 (13.2–20.9)	21.5 (18.2–24.2)
V2H (baseline home)	3.82 (2.40–5.55)	3.60 (2.22–5.30)	37.9 (23.9–57.1)	60.9 (38.8–80.5)
V2H (heat pump)	4.56 (3.34–6.02)	4.06 (2.75–5.66)	43.5 (28.9–63.4)	85.3 (59.6–107)

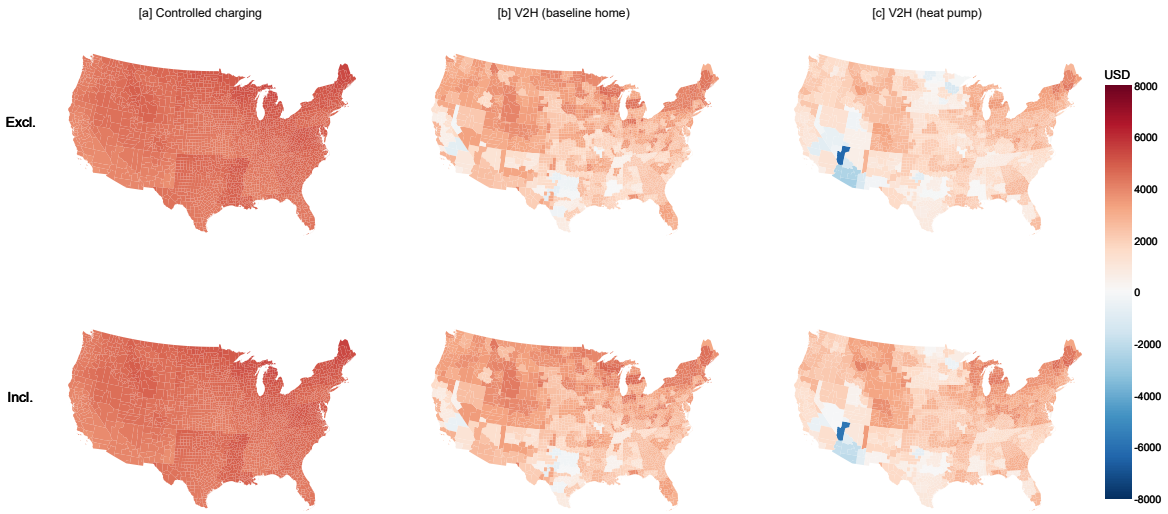


Figure A.23: **Comparison of lifetime charging costs, excluding or including GHG externalities in charging optimization.** Median lifetime charging costs for **a,** controlled charging; **b,** V2H (baseline home); **c,** V2H (heat pump home). Charging costs are defined as the changes to the household's total electricity costs relative to a no-EV counterfactual. Results in the Excl. row assume that the objective function includes only the households' electricity cost. Results in the 'Incl.' row assume that the objective function is the sum of electricity costs and monetized GHG externalities. V2H (baseline home) refers to homes that are representative of the current housing stock, and V2H (heat pump home) refers to fully electrified homes. Map GeoJSON from Plotly visualization tool[58].

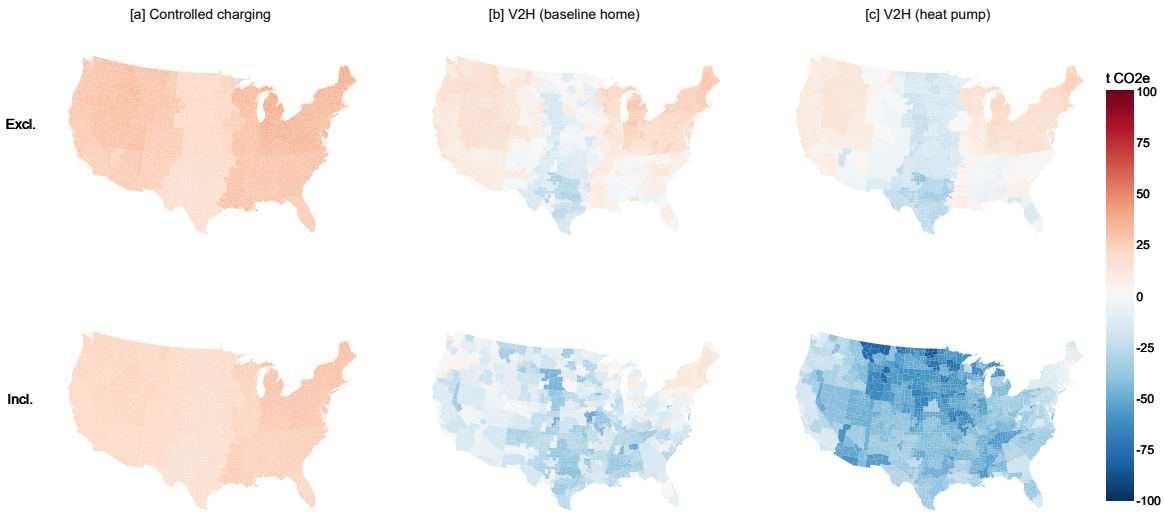


Figure A.24: **Comparison of life-cycle emissions, excluding or including GHG externalities in charging optimization.** Median life-cycle emissions for **a,** controlled charging; **b,** V2H (baseline home); **c,** V2H (heat pump home). Charging emissions are defined as the marginal changes to GHG emissions associated with all the household's electricity purchases relative to a no-EV counterfactual. Results in the Excl. row assume that the objective function includes only the households' electricity cost. Results in the 'Incl.' row assume that the objective function is the sum of electricity costs and monetized GHG externalities. V2H (baseline home) refers to homes that are representative of the current housing stock, and V2H (heat pump home) refers to fully electrified homes. Map GeoJSON from Plotly visualization tool[58].

For controlled charging, cost savings are similar regardless of whether monetized GHG externalities included in the objective function. GHG emission reductions from controlled charging increase by 16-38% relative to a baseline when monetized externalities are accounted for. For V2H in homes with heat pumps, cost savings decrease by 6.0-18% relative to a baseline when monetized GHG externalities are accounted for in deciding when and how much to charge, but the corresponding increase in emission reductions is 70–106%. (see Supplementary Table A.4).

In the base case, EV batteries are cycled for V2H almost as much as for driving, but including GHG externalities in charging optimization increases battery cycling by 2-3 times in the unconstrained V2H case; i.e. batteries undergo many more cycles for V2H than they do for driving. In constrained V2H including GHG externalities in charging optimization increase the number of annual EFCs from about 1/3 of that of driving to 1/2 (see Supplementary Figure A.26).

When GHG externalities are included in charging optimization, the second worst degradation increase caused by switching to V2H from uncontrolled charging in heat pump homes, on average across the contiguous US, is 3.5 percentage points (5th-95th percentile range across regions: 1.4 to 6.0 percentage points, see (Supplementary Figure A.25). The increased capacity loss caused by including GHG emissions in optimization is lower than 7.5 percentage points other than few outliers.

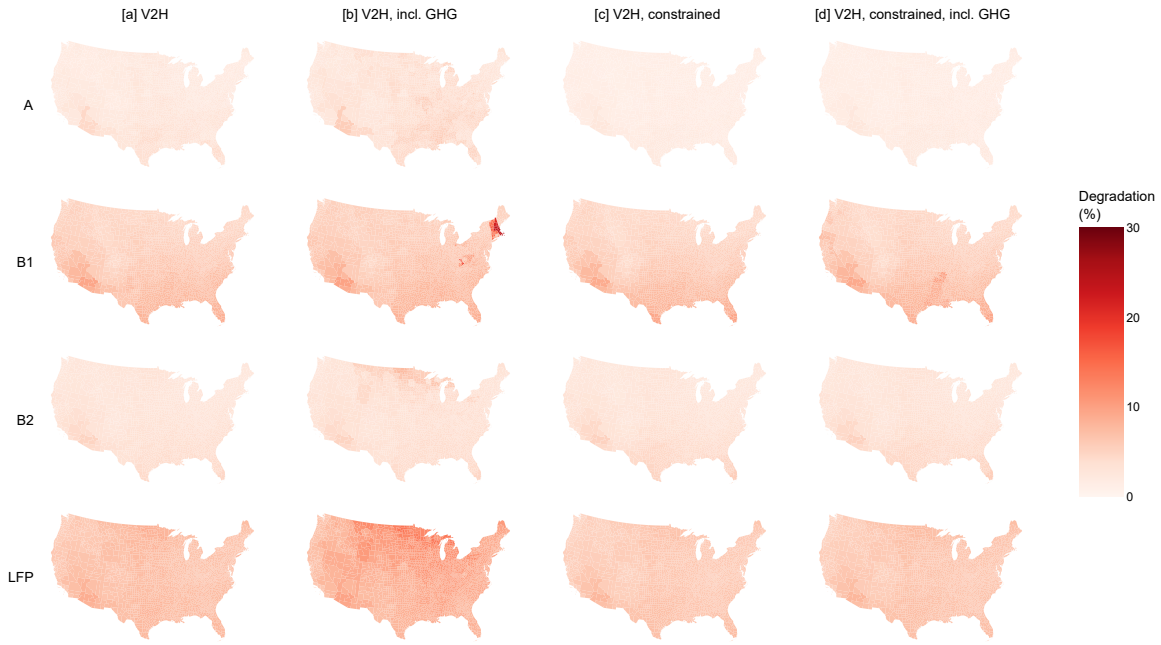


Figure A.25: **Battery degradation across battery and charging scenarios for the case where GHG externalities are part of the objective function.** Second-to-worst capacity loss at the end of 15-year EV lifetime of counties across the US, across battery models for **a,** uncontrolled charging, **b,** controlled charging, **c,** V2H (heat pump), **d,** V2H, constrained. Row headings refer to different cell chemistries, as described in Supplemental Table 3. A, B1, and B2 are Nickel Magnesium Cobalt Oxide (NMC) cells; LFP is a lithium iron phosphate cell. The battery size of the EV is assumed to be 82kWh. All cases are assumed to be baseline homes. 'incl. GHG' means GHG externalities are included in the charging optimization. In 'V2H, Constrained', V2H discharging is limited at 5kW instead of 10kW in the base case. Map GeoJSON from Plotly visualization tool[58].

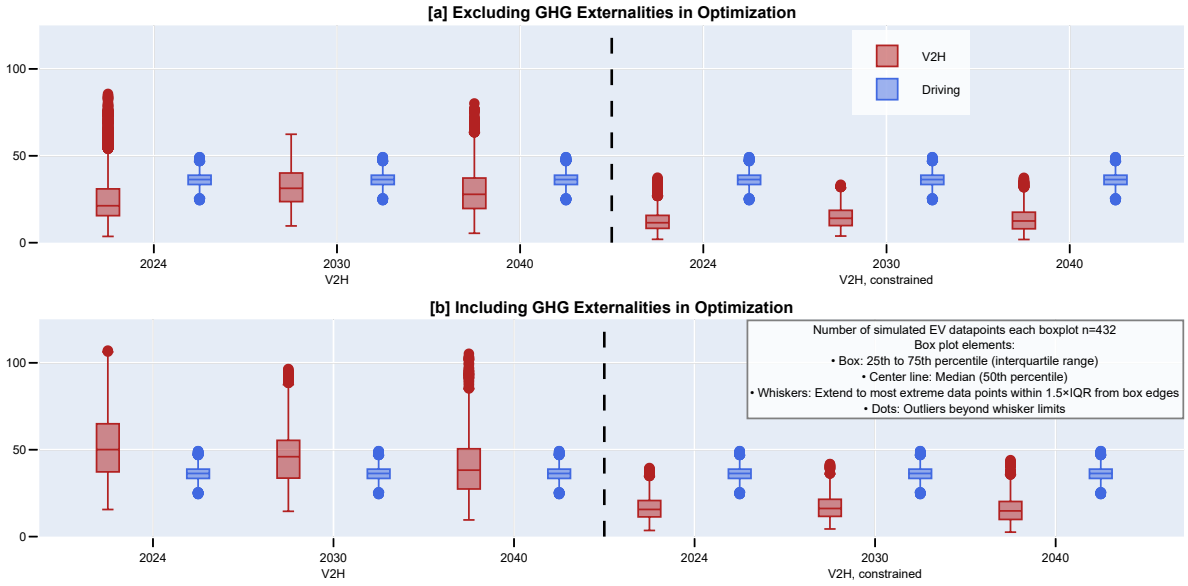


Figure A.26: **Effect of V2H on battery cycling.** Distribution of regional median annual battery full equivalent cycles for V2H (excluding driving) and driving in three modeled years, for V2H and V2H, Constrained. **a,** monetized GHG externalities excluded from charging optimization, and **b,** monetized GHG externalities included in optimization. All cases are assumed to be heatpump homes. In 'V2H, Constrained', V2H discharging is limited at 5kW instead of 10kW in the base case.

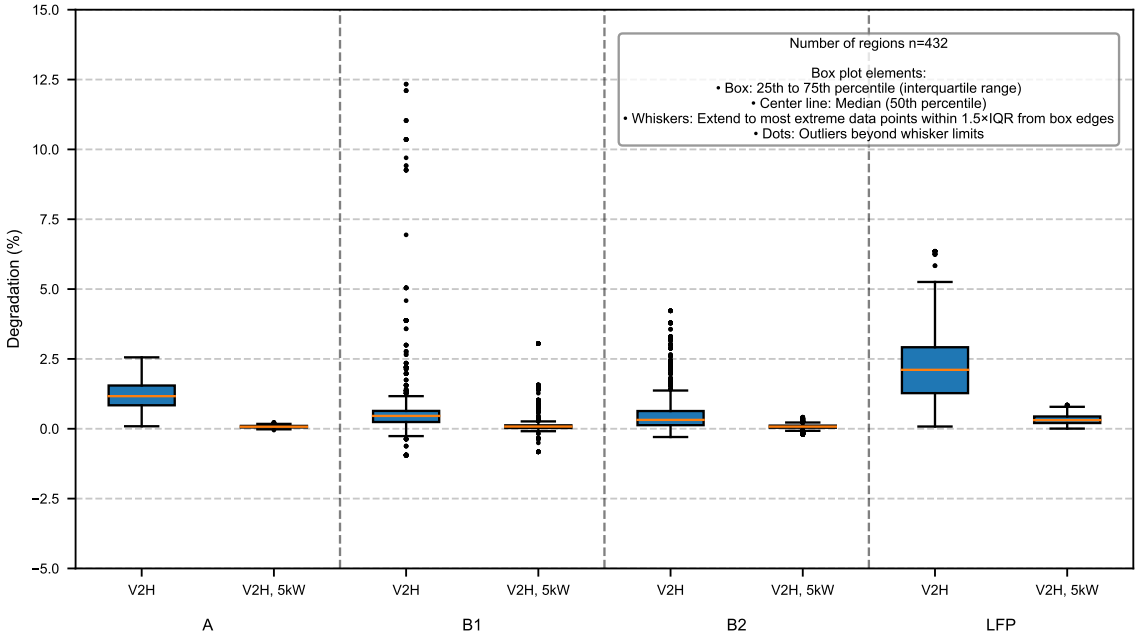


Figure A.27: **Change in second-to-worst capacity loss caused by including GHG externalities in charging optimization.** Change in second-to-worst degradation increase (in percentage points of capacity loss), caused by including GHG externalities in charging optimization, at the end of 15-year EV lifetime of counties across the US, across EV charging behavior cases, and across battery models. All cases are assumed to be baseline homes. In 'V2H, Constrained', V2H discharging is limited at 5kW instead of 10kW in the base case.

A.4.2 Sensitivity: using actual utility rate structures

Our baseline assumption is that EV owners, perhaps through an intermediary, are exposed to hourly fluctuations of electricity prices. We demonstrate here in two cases the differences in outcomes between this baseline assumption and examples of current utility rates.

We chose two sets of comparisons for this case study: a time-of-use rate program offered by DTE in Southeast Michigan and a constant rate program offered in many parts of the country. Under a constant rate structure which does not have hourly fluctuations in electricity prices, there are no cost benefits from V2H because there is nothing to be gained from shifting load. For time-of-use rates, Supplementary Figure A.28 shows cost and emissions reductions under a time-of-use rate (Residential Time of Day (Full Service)-D1.2, retrieved on Jan 01 2025). V2H can reduce costs but not reduce emissions, since the low-cost hours have high marginal emissions in this region. The caveat with this analysis is that it represents the rate structure that prevails today, and provides limited insight about the benefits and costs of V2H over the lifetime of a vehicle purchased today.

A.4.3 EVs with smaller batteries

We assessed the lifetime charging costs, GHG emissions, and battery health loss in the lifetime of a hypothetical EV with a 60 kWh battery capacity. All other factors are kept the same.

A.4.3.1 Charging costs

Adding EV charging to baseline electricity consumption increases lifetime electricity bills by an average of $8600 (5th percentile increase of $7400 in South Nevada; 95th percentile increase of $9800 in Kentucky) with uncontrolled charging. With controlled charging,

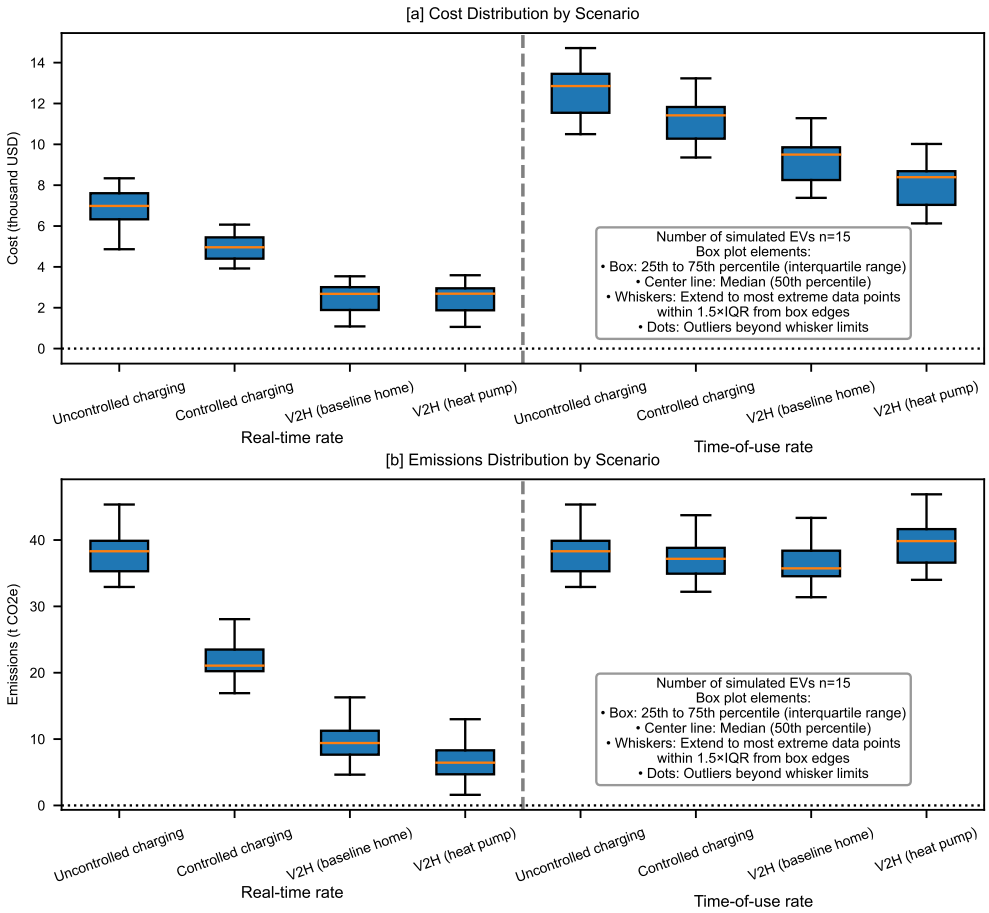


Figure A.28: **Effect of using real-world utility rates on charging costs and emissions.** Vehicle **a,** lifetime charging costs and **b,life-cycle** emissions under DTE's Residential Time of Day (Full Service)-D1.2 and under real-time prices (base case assumption).

bills increase by an average of $5900 (5th percentile increase of $4800 in Texas; 95th percentile increase of $7000 in New York). With V2H integration, EV charging increases electricity bills by an average of $770 over the 15-year lifetime of the EV (5th percentile increase of $-1200 in Texas; 95th percentile increase of $2900 in Michigan). Allowing V2H integration substantially reduces the cost of EV charging by an average of 91% (5th percentile reduction of 70% in Ohio; 95th percentile reduction of 120% in Florida) (see Supplementary Figure A.29 and Supplementary Figure A.30).

Overall, costs are higher for EVs with 60-kWh batteries compared with EVs with 82-

kWh batteries. As EVs with 60kWh batteries need to rely on fast charging (150kW) more to cover driving demands. However, EV-system integration, especially V2H, can still reduce charging costs significantly compared with uncontrolled charging, though the savings are less than EVs with 80kWh batteries. This is because fast charging is more expensive than slow charging at home or work. Moreover, fast charging cannot be rescheduled like slow charging and hence does not respond to price signals.

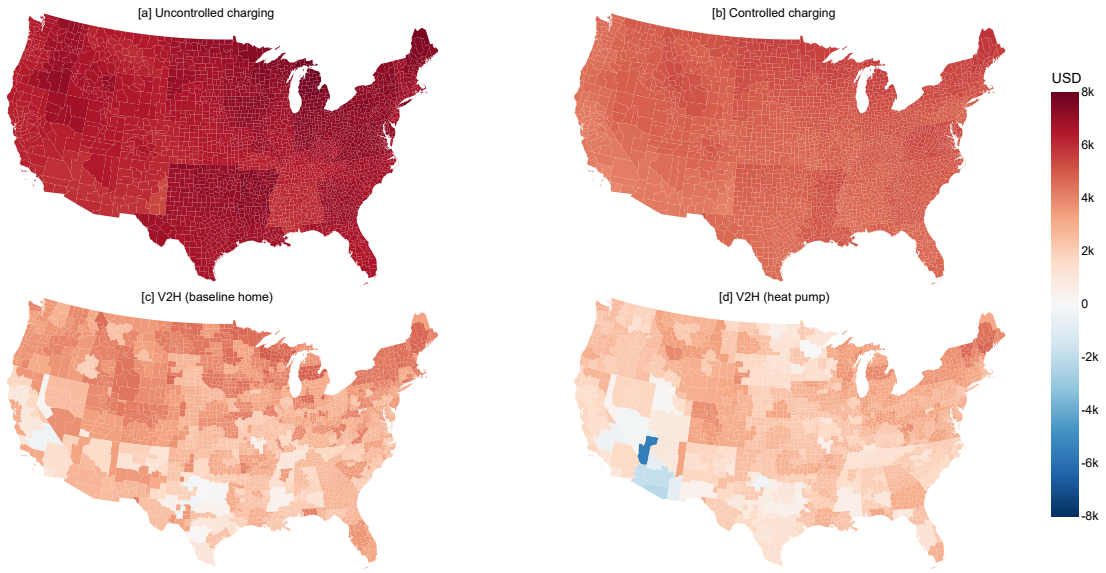


Figure A.29: **Median lifetime EV charging costs across charging scenarios for a vehicle with a 60kWh battery.** Median lifetime charging costs for the representative EV with, **a,** uncontrolled charging, **b,** controlled charging, **c,** V2H in baseline homes, **d,** and V2H in homes with whole-home electrification (in short referred to as 'V2H (heat pump)', because heat pumps dominate load changes in whole-home electrification). Charging costs are defined as the cost changes to the household's total electricity bills relative to a no-EV counterfactual. 'V2H' is short for vehicle-to-home. The EV battery capacity is 60 kWh; compare with results in Figure 2 for the baseline vehicle with an 82kWh battery. Map GeoJSON from Plotly visualization tool[58].

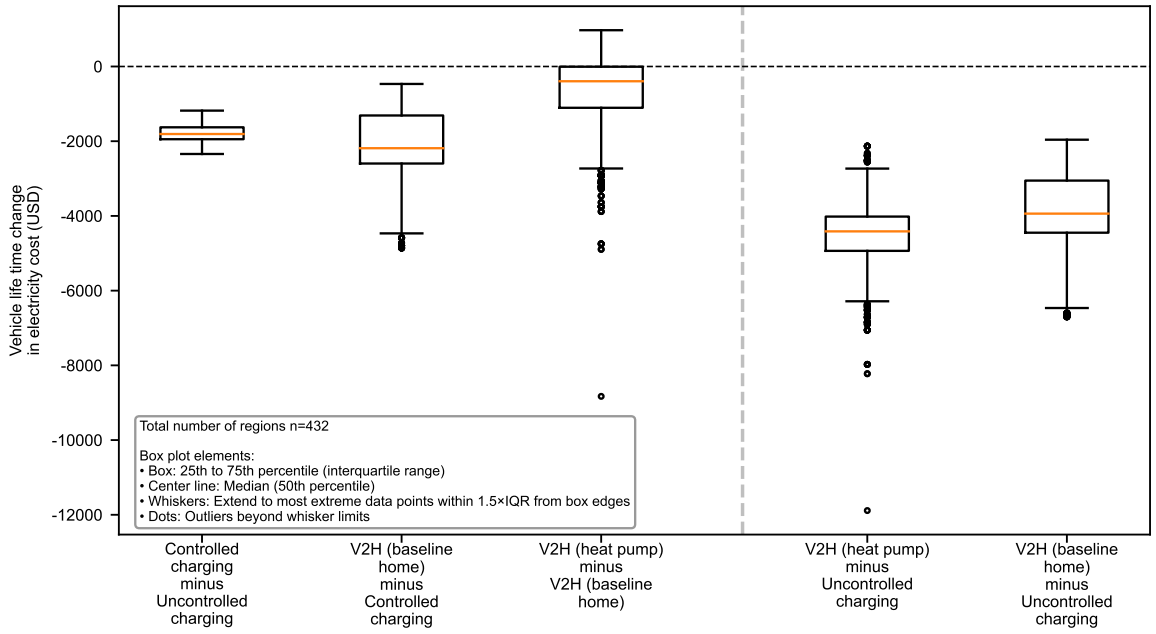


Figure A.30: **Distribution of differences in median lifetime charging costs of EVs under different charging scenarios for a vehicle with a 60kWh battery.** Each data point represents the median difference for one RGU. Charging costs are defined as a net increase in electricity bills for the whole home relative to a no-EV counterfactual. 'V2H' is short for vehicle-to-home; 'RGU' is short for reference geographical unit. Results are for a vehicle with a 60kWh battery; compare with results in Figure 2 for the baseline vehicle with an 82kWh battery.

A.4.3.2 GHG emissions

Compared with ICEV, EVs with smaller batteries using uncontrolled charging reduce lifetime GHG emissions of the operational stage everywhere in the contiguous US (see Supplementary Figure A.31 and Supplementary Figure A.32). The average lifetime emissions of EVs are $29tCO_2e$, lower than similar-sized ICEVs ($59tCO_2e$). The average relative emission reduction is 50% (5th percentile of 38% in Indiana, 95th percentile of 65% in Texas).

Controlled charging and V2H both reduce charging emissions significantly across the US. Adding EV charging to baseline electricity consumption increases lifetime electricity emissions by an average of 29 tCO_2e (5th percentile increase of 22 tCO_2e in California; 95th percentile increase of 38 tCO_2e in Ohio) with uncontrolled charging. With con-

trolled charging, emissions increase by an average of $9.2tCO_2e$ (5th percentile increase of $2.8tCO_2e$ in Texas; 95th percentile increase of $16tCO_2e$ in Ohio). With V2H integration, EV charging **reduces** electricity emissions by an average of 43 tCO_2e over the 15-year lifetime of the EV (5th percentile reduction of 23 tCO_2e in California; 95th percentile reduction of $62tCO_2e$ in North Dakota). For uncontrolled charging, the annual charging emissions are reduced significantly with grid decarbonization from 2024 to 2040, even though uncontrolled charging does not respond to monetized emission factor signals.

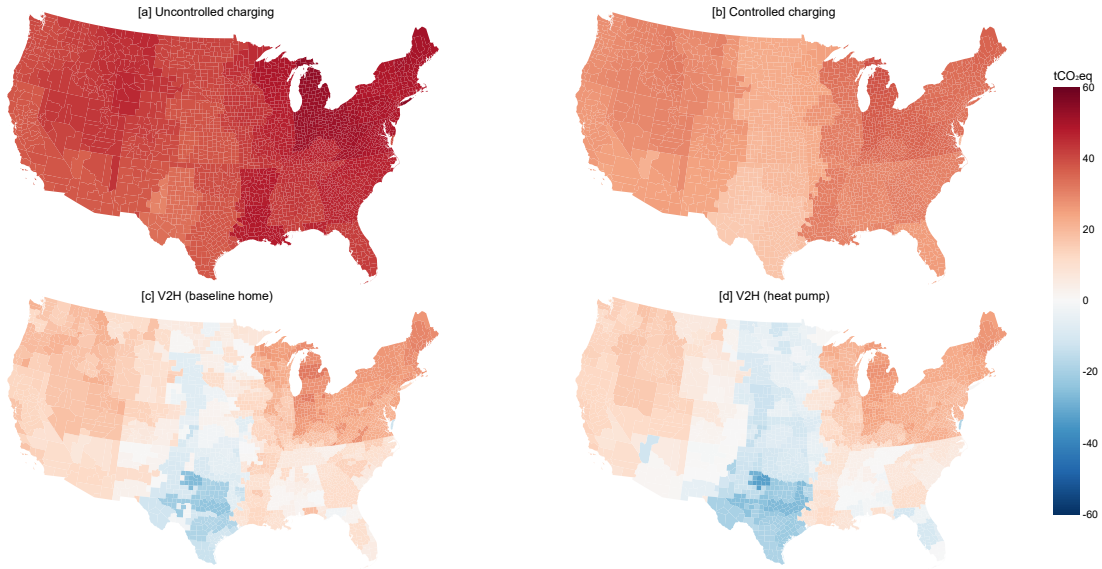


Figure A.31: **Median EV life-cycle greenhouse gas emissions across charging scenarios for a vehicle with a 60kWh battery.** Median life-cycle greenhouse gas emissions for the representative EV with **a,** uncontrolled charging, **b,** controlled charging, **c,** V2H in baseline homes, **d,** and V2H in homes with whole-home electrification (in short referred to as 'V2H (heat pump)', because heat pumps dominate load changes in whole-home electrification). Charging emissions are defined as the changes to the household's total electricity-related emissions to a no-EV counterfactual. 'V2H' is short for vehicle-to-home. Map GeoJSON from Plotly visualization tool[58].

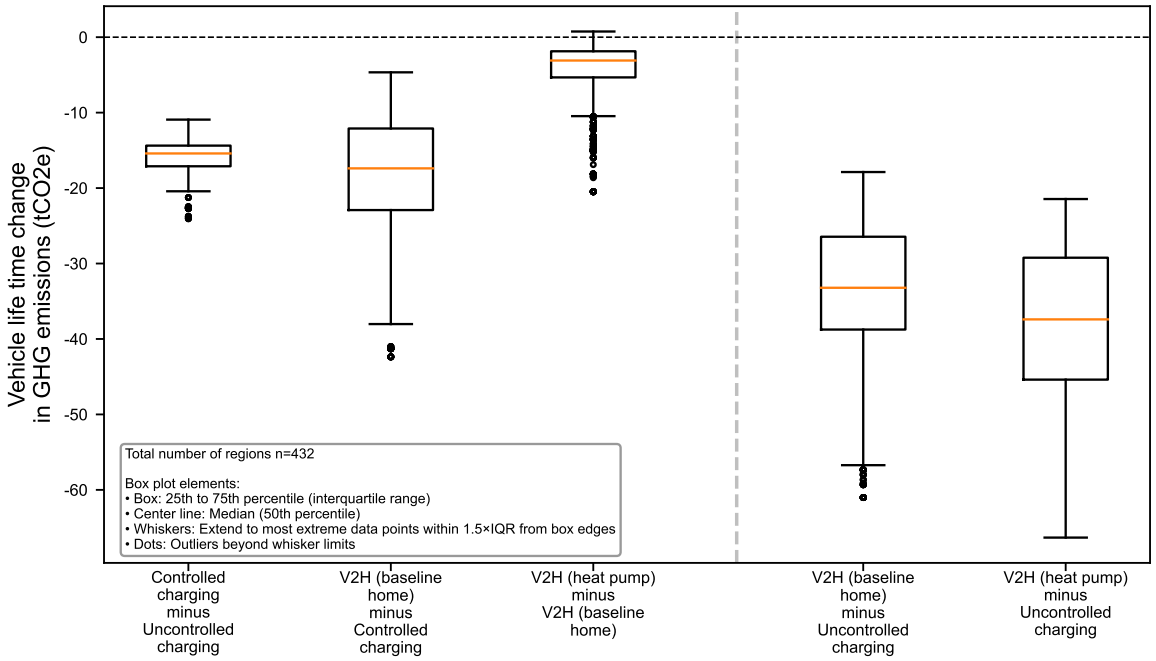


Figure A.32: **Distribution of changes in median lifetime charging greenhouse gas emissions of EVs under different charging scenarios for a vehicle with a 60kWh battery.** Each data point represents the median difference for one RGU. Charging costs are defined as a net increase in electricity bills for the whole home relative to a no-EV counterfactual. 'V2H' is short for vehicle-to-home; 'RGU' is short for reference geographical unit. Results are for a vehicle with a 60kWh battery; compare with results in Figure 2 for the baseline vehicle with an 82kWh battery.

The estimated vehicle-cycle emissions of a medium-sized SUV are 8.03tCO_2e for ICEVs, 8.42tCO_2e for HEVs, and 11.3tCO_2e for EVs with 60kWh batteries. Despite higher vehicle-cycle emissions, EVs have lower life-cycle emissions than ICEVs everywhere in the US (9.7-28tCO_2e, 90th percentile range of emission reduction). EVs have lower life-cycle emissions than HEVs in coastal WECC and southern states (0–14tCO_2e difference), whereas HEVs have lower life-cycle emissions in the rest of the country (0–3.7tCO_2e difference).

A.4.3.3 Battery capacity loss

Supplementary Figure A.34 and Supplementary Figure A.33 depict the degradation and degradation changes across battery cells and charging operations. 'NMC B1' sees a

decrease in degradation with V2H. The average decrease in degradation is 3.6 percentage points of capacity loss (90th percentile range: 2.6–4.9% of capacity loss). 'NMC A' has the highest increase in degradation due to V2H. The average change in degradation is 3.6 percentage points of capacity loss (90th percentile range: 1.9–5.4% of capacity loss).

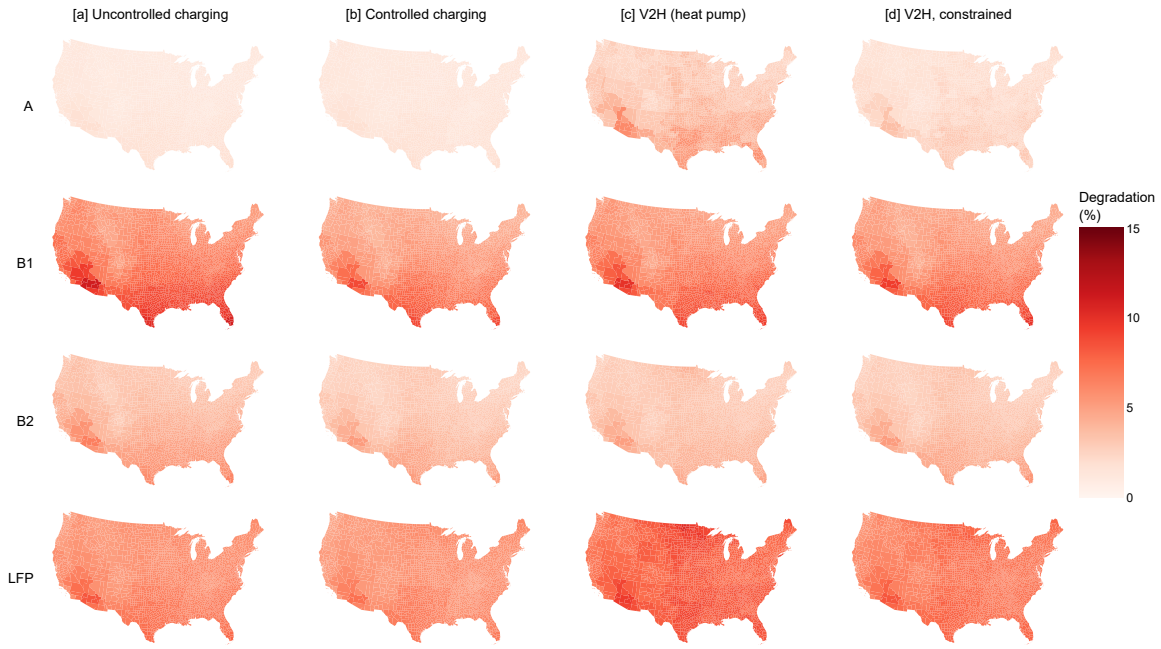


Figure A.33: **Battery degradation across battery and charging scenarios for a vehicle with a 60kWh battery.** Second-to-worst capacity loss at the end of 15-year EV lifetime of counties across the US, across battery models for **a,** uncontrolled charging, **b,** controlled charging, **c,** V2H (heat pump), **d,** V2H, constrained. Row headings refer to different cell chemistries, as described in Supplemental Table 3. A, B1, and B2 are Nickel Magnesium Cobalt Oxide (NMC) cells; LFP is a lithium iron phosphate cell. The battery size of the EV is assumed to be 60kWh; compare with the results in Supplementary Figure 2 for a baseline vehicle with an 82kWh battery. Deeper red indicates higher capacity loss. Map GeoJSON from Plotly visualization tool[58].

A.4.4 Emission assessment with grid average emission rates

Here we assess the sensitivity of our results to an alternative modeling strategy: using hourly average emissions rates (AERs). The use of AERs does not affect our optimization when the objective function includes only the charging costs, but does affect our estimates of emissions reductions.

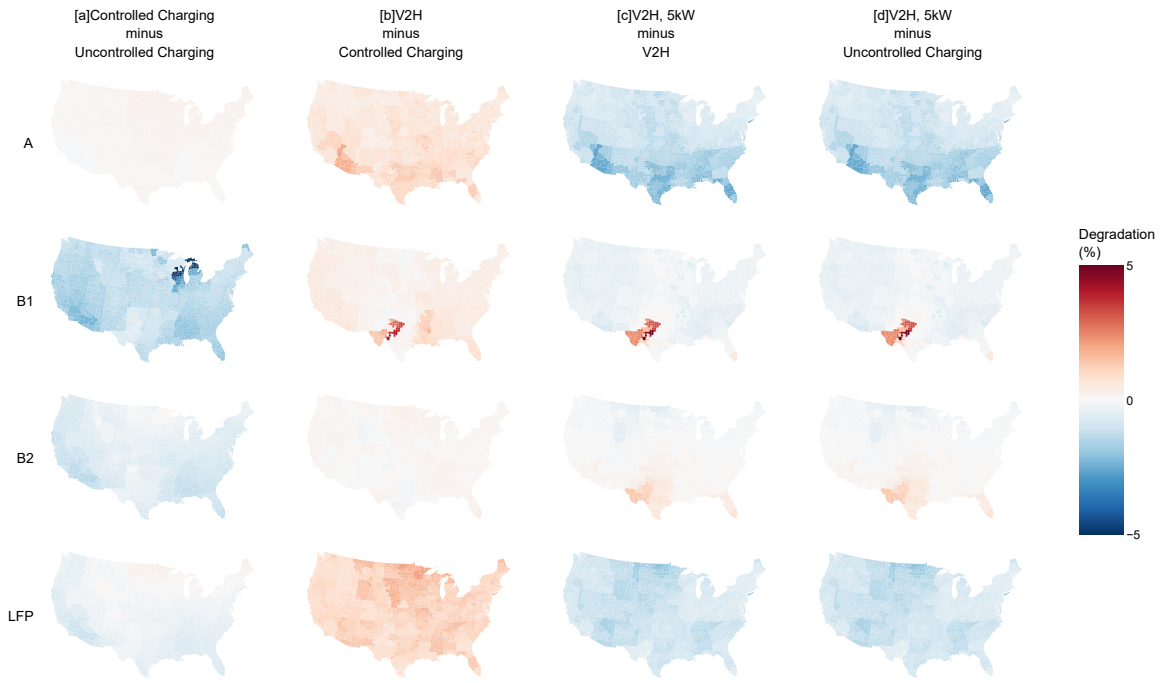


Figure A.34: **Increase in capacity loss due to different charging strategies for a vehicle with a 60kWh battery.** Change in second-to-worst capacity loss (in percentage points of capacity loss), caused by charging strategies, at the end of 15-year EV lifetime for different battery chemistries for **a,** controlled charging minus uncontrolled charging, **b,** V2H minus controlled charging, **c,** V2H, constrained minus V2H, **d,** V2H, constrained minus uncontrolled charging. Row headings refer to different cell chemistries, as described in Supplemental Table 3. A, B1, and B2 are Nickel Magnesium Cobalt Oxide (NMC) cells; LFP is a lithium iron phosphate cell. Results are labeled as "<Scenario 2> minus <Scenario 1>". Positive, red values indicate that going from Scenario 1 to 2 produces a worse outcome (more capacity loss), while negative, blue values indicate an improvement (less capacity loss). The battery size of the EV is assumed to be 60kWh; compare with the results in Supplementary Figure 3 for a baseline vehicle with an 82kWh battery. Map GeoJSON from Plotly visualization tool[58].

Emissions of EVs with uncontrolled charging are much lower when assessed with AERs than MERs. This is because during evening EV charging, low-emitting renewable (e.g., wind) or firm (e.g., nuclear) generators are not at the margin, but still contributing to the generation mix. So, MERs are high, while AERs are lower. Supplementary Figure A.35 and Supplementary Figure A.36 show that controlled charging and V2H still reduce emissions compared with uncontrolled charging, ICEVs and HEVs. However, our central conclusions hold: V2H yields greater emissions savings than does controlled charging, and there are small synergies between V2H and home electrification.

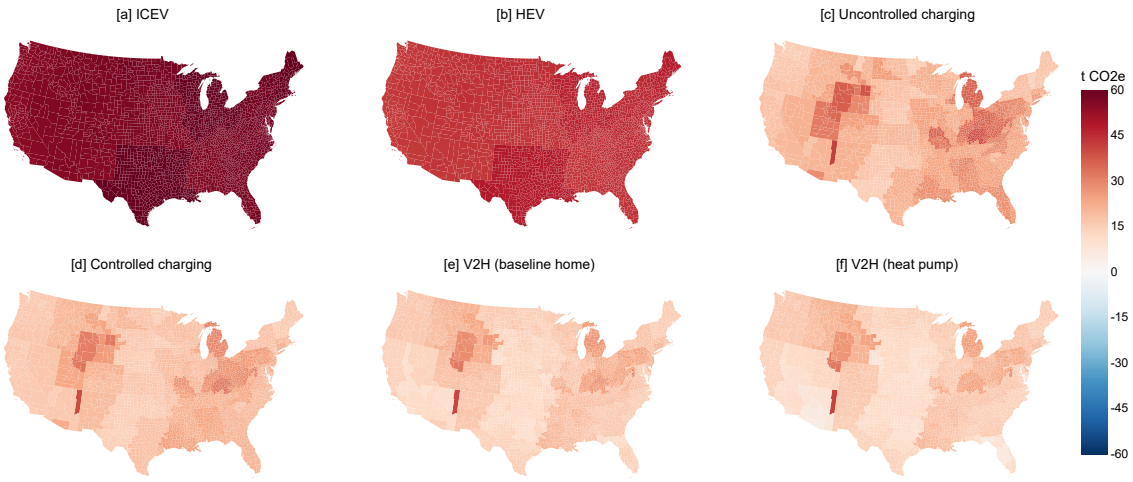


Figure A.35: **Median life-cycle greenhouse gas emissions across drivetrains and EV charging scenarios assuming hourly average emissions rates for electricity generation.** Median life-cycle GHG emissions for mid-sized SUVs, including **a,** ICEVs, **b,** HEVs , **c,** EVs with uncontrolled charging, **d,** EVs with controlled charging, **e,** EVs with V2H in baseline homes, **f,** EVs with V2H in homes with heat pumps for heating. Emissions for V2H scenarios represent the change in emissions from all household electricity uses relative to a no-vehicle counterfactual. 'V2H' is short for vehicle-to-home; 'ICEV' is short for internal combustion engine vehicle; 'HEV' is short for hybrid electric vehicle. Compare with Figure 4 for the base case in which we use hourly short-run marginal emissions. Map GeoJSON from Plotly visualization tool[58].

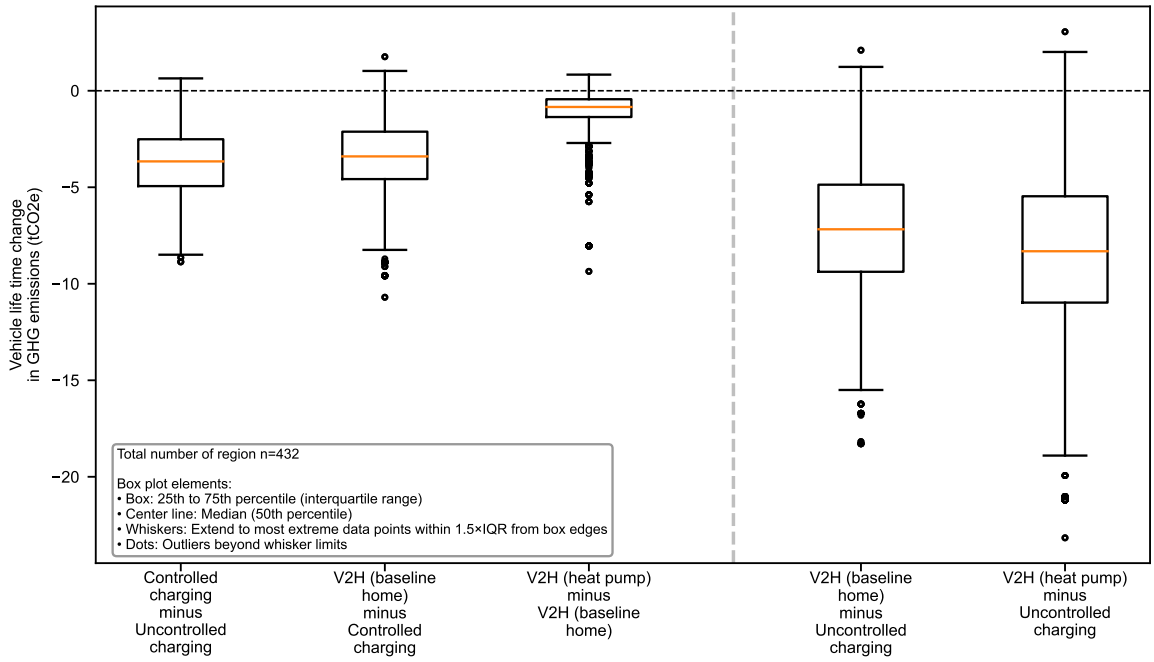


Figure A.36: **Distribution of median differences in life-cycle emissions of EVs under different charging scenarios assuming hourly average emissions rates for electricity generation.** Each data point represents the median difference for one RGU. The box extends from the 1st to the 3rd quartile of the data, with a line at the median. The whiskers extend from the box to the farthest data point lying within 1.5x the inter-quartile range from the box. Charging emissions are defined as the net increase in total GHG emissions of the whole home compared to a no-EV counterfactual. 'V2H' is short for vehicle-to-home. Compare with Figure 4 for the base case in which we use hourly short-run marginal emissions.

A.4.5 Complete results of the sensitivity case with GHG externalities in charging optimization

We find that, on average, for the representative EV, controlled charging yields a vehicle lifetime cost reduction of $1.7k (5th-95th percentile range: $1.4k–$2.0k), or 27% (22%-32%) and a vehicle lifetime GHG emissions reduction of 21tCO_2e (18tCO_2e–24tCO_2e), or 74% (61%-93%) relative to an uncontrolled charging baseline. In the rest of the paper, 'lifetime' refers to *vehicle* lifetime, which we assume is 15 years. Homes representative of the current housing stock, which use a mix of electricity and fossil fuels for different end uses (referred to as 'baseline homes'), see an average lifetime V2H cost reduction of $3.6k ($2.2k–$5.3k), or 58% (35%-88%) and an average lifetime emission reduction of 61tCO_2e (39tCO_2e-80tCO_2e), or 210% (120%-320%). Reductions exceed 100% because V2H-enabled reductions in emissions from other household electricity purchases exceed vehicle charging emissions. In contrast, for homes in which all end uses are electrified (referred to as 'heat pump' homes), the average lifetime V2H cost reductions are $4.1k ($2.8k–$5.7k), or 65% (44%-91%), with an average lifetime emission reduction of 85tCO_2e (60tCO_2e–107tCO_2e), or 300% (200%-420%). We find that there are modest GHG reduction synergies between full electrification (i.e., using electricity for all domestic end uses) and V2H in most places in the US. While our modeling suggests that V2H does not substantially increase battery capacity loss, more work is needed to confirm this finding (see Supplementary Result Section A.4.5.3 for battery degradation)

A.4.5.1 EV charging costs

Supplementary Figure A.37 maps the lifetime charging costs of the representative EV. In this case, with uncontrolled charging, adding EV charging to household electricity consumption increases lifetime electricity bills by $6.3k ($5.7k–$6.9k). In comparison, lifetime fuel costs internal combustion engine vehicles (ICEVs) are $16.3k ($15.5k-$17.7k), those of hybrid electric vehicles (in short as 'HEV') are $12k ($11k–$13k) (detailed method description in Supplementary Method Section on gasoline vehicle modeling.

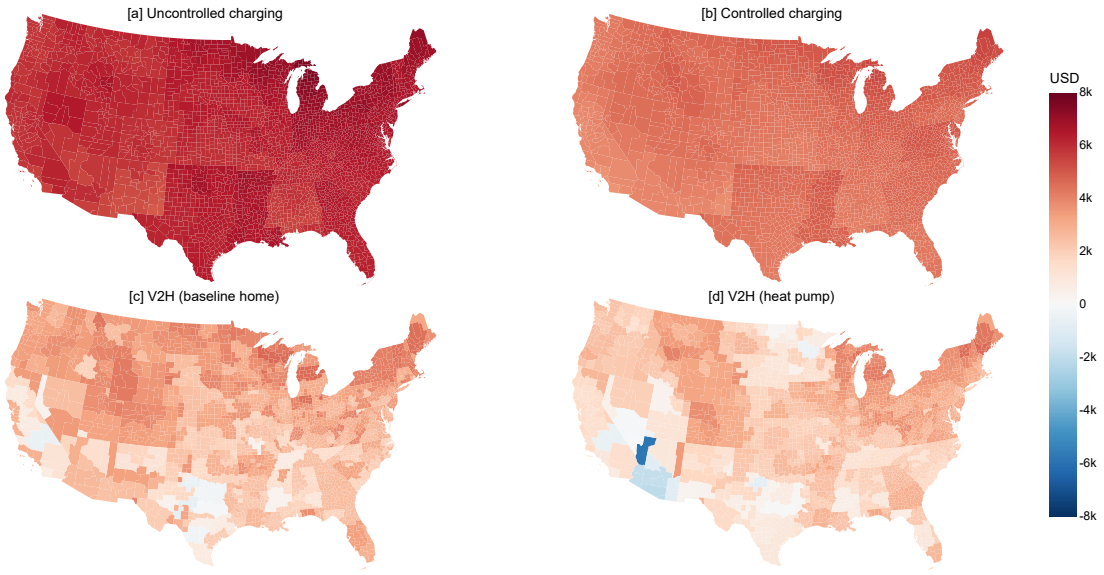


Figure A.37: **Median lifetime EV charging costs across charging scenarios with GHG externalities in the objective function.** Median lifetime charging costs for the representative EV with, **a,** uncontrolled charging, **b,** controlled charging, **c,** V2H in baseline homes, **d,** and V2H in homes with whole-home electrification (in short referred to as 'V2H (heat pump)', because heat pumps dominate load changes in whole-home electrification). Charging costs are defined as the cost changes to the household's total electricity bills relative to a no-EV counterfactual. 'V2H' is short for vehicle-to-home. Compare with Figure 2, with results for the baseline case in which we optimize only for cost. Map GeoJSON from Plotly visualization tool[58].

Grid decarbonization increases the number of hours when electricity sources with low marginal costs (e.g., wind and solar) are at the margin. Controlled charging allows owners to shift EV charging demand to hours in which electricity prices are low [59]. V2H integration allows owners to shift other household energy use, producing an even larger gain.

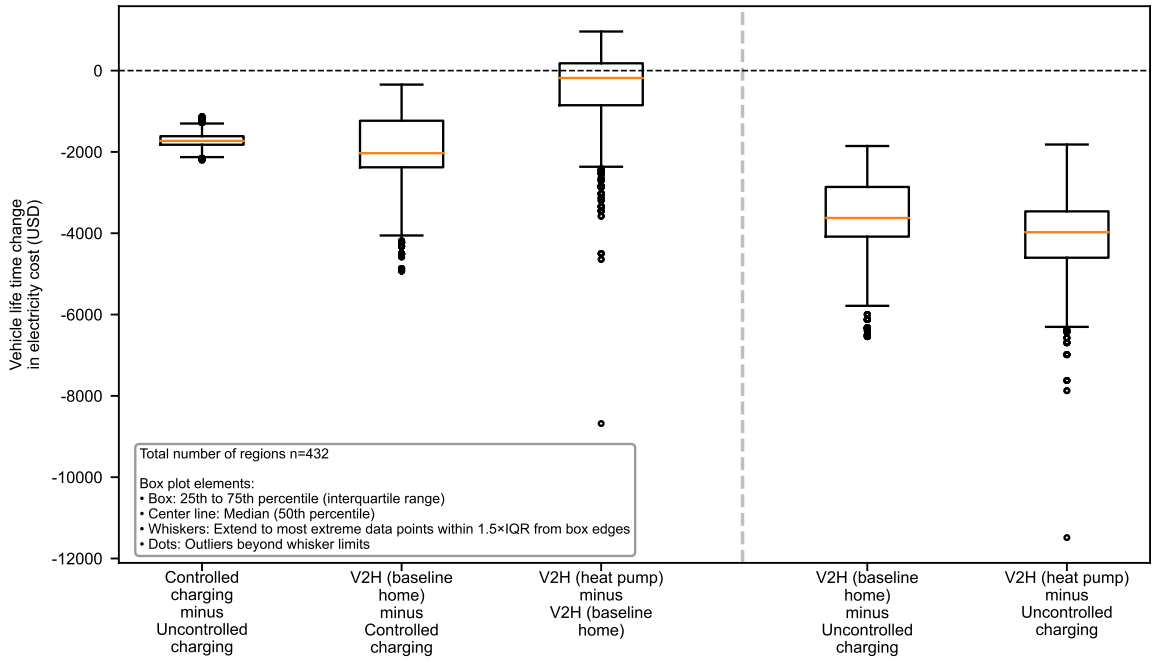


Figure A.38: **Distribution of median differences in lifetime charging costs of EVs under different charging scenarios with GHG externalities in the objective function.** Each data point represents the median difference for one RGU. Charging costs are defined as a net increase in electricity bills for the whole home relative to a no-EV counterfactual. 'V2H' is short for vehicle-to-home; 'RGU' is short for reference geographical unit. Compare with Figure 3, with results for the baseline case in which we optimize only for cost.

Consequently, controlled charging and V2H reduce lifetime electricity bills in the contiguous United States (as shown in Supplementary Figure A.38). Relative to uncontrolled charging, the cost reduction by controlled charging, averaged over the 432 regions, is \$1.7k (\$1.4k-\$2.0k), or 27% (22%-32%). For baseline homes, V2H integration reduces the lifetime electricity costs by an average of \$3.6k (\$2.2k-\$5.3k), 58% (35%-88%). In contrast, V2H in homes with whole-home electrification see an average lifetime cost reduction of \$4.1k (\$2.8k-\$5.7k), or 65% (44%-91%) compared with uncontrolled charging. In Texas and parts of California, V2H in baseline homes reduces the cost of electricity so much that the reduction exceeds the cost of charging the vehicle. In homes with heat pumps, which also provide more efficient air conditioning than currently installed air conditioners, V2H savings would exceed charging costs in parts of the Upper Midwest, Arizona, and Nevada, in addition to California and Texas.

There are small synergies between heat pump adoption and V2H in most places, the average change in costs is $450 (-460–2400USD) (see Supplementary Figure A.38. If the solutions presented here were true optima, V2H savings from heat pump homes would always be at least as great as those from baseline homes. However, V2H under-performs in heat pump homes in 143 out of 432 regions because the optimization algorithm has limited foresight and therefore does not guarantee an optimal solution over the whole year.

A.4.5.2 EV charging emissions

With uncontrolled charging, EVs have lower **life-cycle** emissions than ICEVs everywhere in the US (14t CO_2e lower on average, 5th to 95th percentile range of 7.6–25tCO_2e). HEVs have similar or lower **life-cycle** emissions than EVs in the Great Lakes and Northeastern US regions, whereas EVs have lower **life-cycle** emissions in the rest of the country (HEVs are 0.93tCO_2e higher on average, with difference ranging -5.7–10.7tCO_2e). EVs with controlled charging have lower emissions than both ICEVs and HEVs everywhere in the US, 22tCO_2e lower than HEVs on average, with a range of 32–17tCO_2e (see Supplementary Figure A.39 and Supplementary Figure A.40).

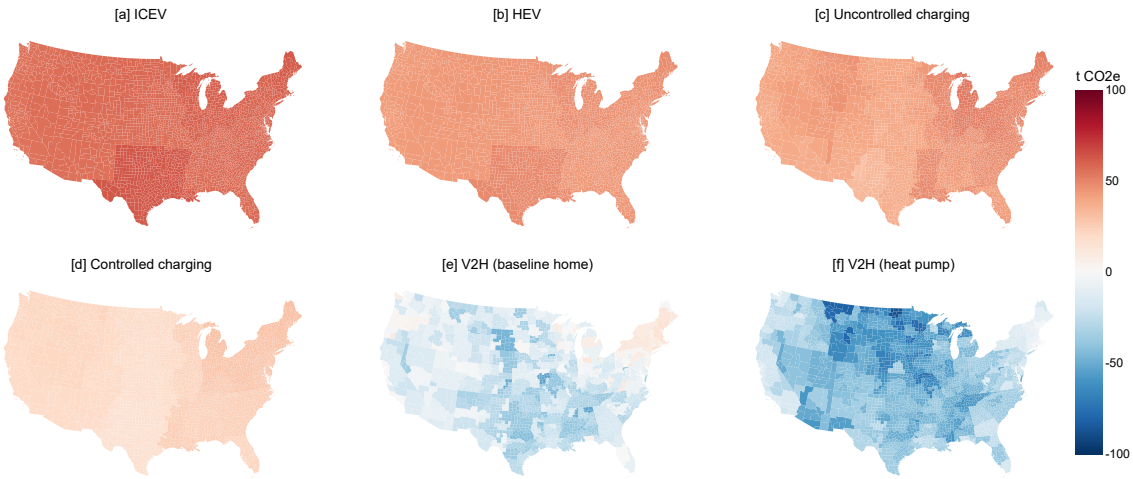


Figure A.39: **Median life-cycle greenhouse gas emissions across drivetrains and EV charging scenarios with GHG externalities in the objective function.** Median life-cycle GHG emissions for mid-sized SUVs, including **a,** ICEVs, **b,** HEVs , **c,** EVs with uncontrolled charging, **d,** EVs with controlled charging, **e,** EVs with V2H in baseline homes, **f,** EVs with V2H in homes with heat pumps for heating. Emissions for V2H scenarios represent the change in emissions from all household electricity uses relative to a no-vehicle counterfactual. 'V2H' is short for vehicle-to-home; 'ICEV' is short for internal combustion engine vehicle; 'HEV' is short for hybrid electric vehicle. Compare with Figure 4, with results for the baseline case in which we optimize only for cost. Map GeoJSON from Plotly visualization tool[58].

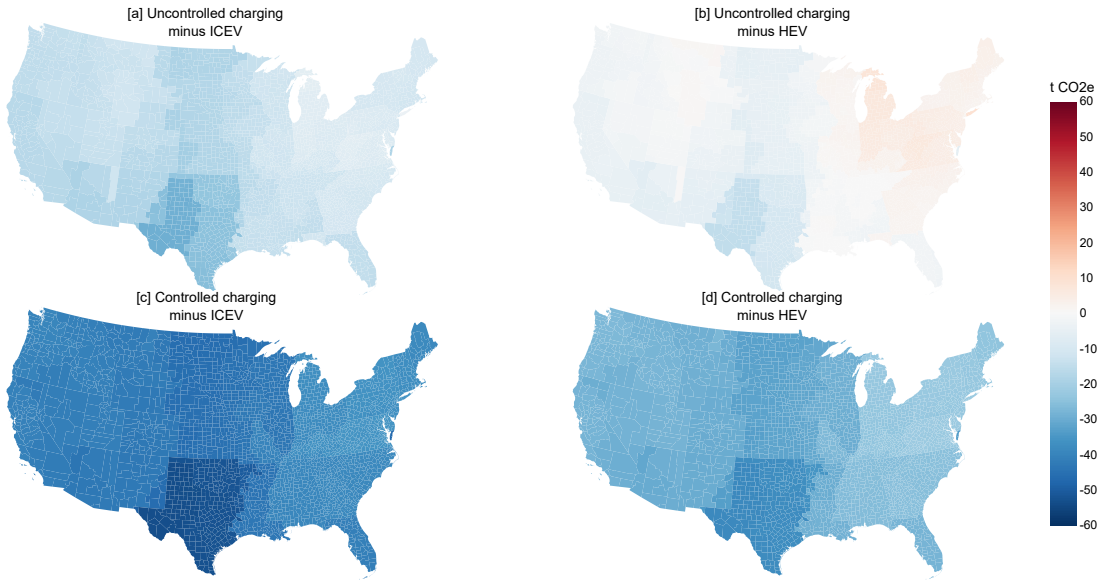


Figure A.40: **Reduction in life-cycle greenhouse gas emissions from switching to EVs from ICEVs and HEVs with GHG externalities in the objective function.** Median differences in life-cycle GHG emissions, between between **a,** EVs with uncontrolled charging and ICEVs, **b,** EVs with uncontrolled charging and HEVs, **c,** EVs with controlled charging and ICEVs, and **d,** EVs with controlled charging and HEVs. 'ICEV' is short for internal combustion engine vehicle; 'HEV' is short for hybrid electric vehicle. Compare with Figure 5, with results for the baseline case in which we optimize only for cost. Map GeoJSON from Plotly visualization tool[58].

As Supplementary Figure A.39 shows, with uncontrolled charging, adding EV charging to baseline electricity consumption increases lifetime electricity emissions by an average 30tCO_2e (5th-95th percentile range of 22–37tCO_2e). With controlled charging, emissions increase by an average of 8tCO_2e (1.5–14tCO_2e). For V2H in baseline homes, V2H savings more than offset charging emissions in most parts of the country (in 99% of counties, covering 98% of the US population), with an average lifetime charging emissions of -31tCO_2e (-53 – -6tCO_2e). In fully electrified homes, V2H emissions reductions exceed charging emissions everywhere across the country, resulting in charging emissions of -56tCO_2e (-79 – -29tCO_2e). Supplementary Figure A.41 shows V2H substantially reduces GHG emissions compared with uncontrolled charging. In baseline homes, average emission reductions are 61tCO_2e (39–80tCO_2e), or 260% (140%-700%). In fully electrified homes, emission reductions are 24tCO_2e (5.1–50tCO_2e), or 44% (13%-83%), higher than in baseline homes, and only in 1 out of 432 regions does V2H in fully electrified homes see higher emissions than in baseline homes, suggesting synergies between building electrification and vehicle electrification with V2H.

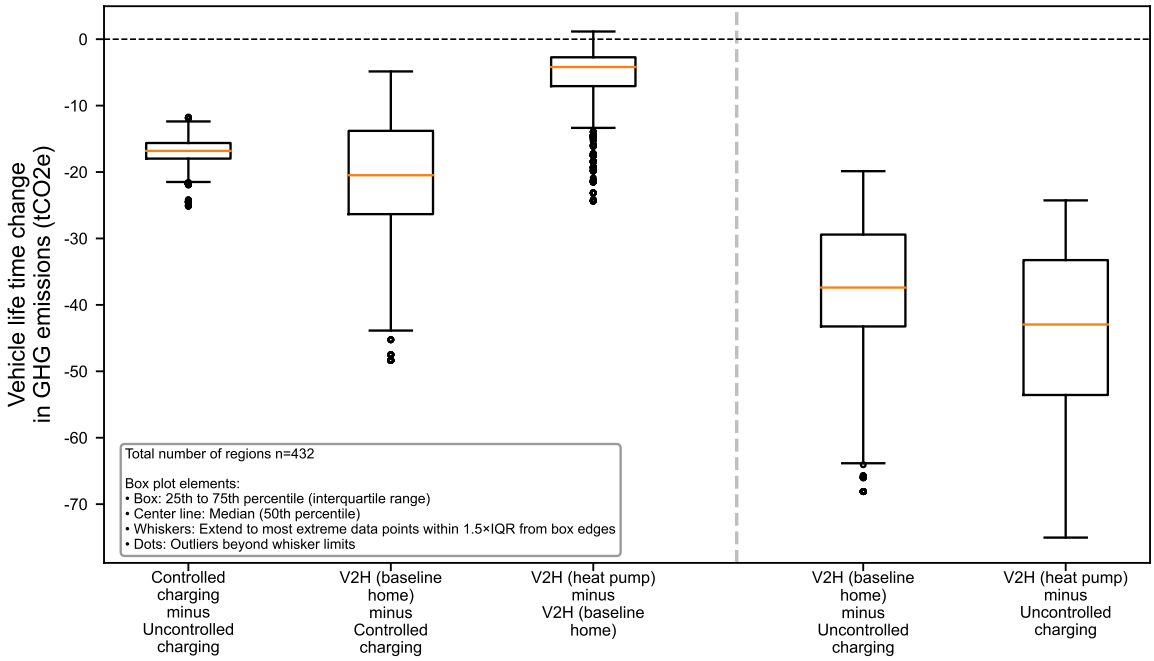


Figure A.41: **Distribution of median differences in life-cycle emissions of EVs under different charging scenarios with GHG externalities in the objective function.** Each data point represents the median difference for one RGU. The box extends from the 1st to the 3rd quartile of the data, with a line at the median. The whiskers extend from the box to the farthest data point lying within 1.5x the inter-quartile range from the box. Charging emissions are defined as the net increase in total GHG emissions of the whole home compared to a no-EV counterfactual. 'V2H' is short for vehicle-to-home. Compare with Figure 2.6, with results for the baseline case in which we optimize only for cost.

A.4.5.3 EV battery capacity loss

V2H more than doubles the number of cycles the battery experiences Supplementary Figure A.26: the number of battery cycles for V2H is almost 1.5 times as many as that for driving. For the vehicle in each region with the second-highest degradation (the results for the worst vehicle are noisy), the additional degradation after 15 years —averaged across the US—is 0.87 percentage points (5th-95th percentile range across regions: 0.37 to 1.6 percentage points). We calculate the cell-level battery degradation using different existing models for cells with different chemistries , but do not comment on the real-world battery degradation which is affected by many factors that we do

not model [50]. Nevertheless, our conclusion that additional battery throughput for the V2H scenario does not substantially increase battery capacity loss is consistent across the cases modeled here, aligning with the findings of recent publications [51], [53], [60].

Nonetheless, customer concerns about battery longevity and manufacturer concerns about warranty costs may mean that restrictions are placed on V2H. If we consider a case in which V2H is restricted to only peak hours and at a discharge rate of no more than 5 kW (instead of 10kW in the base case), battery cycling for V2H is reduced by about 50%. Supplementary Figure A.42 [a] and [b] show that, even with these restrictions, V2H cuts both charging costs and greenhouse emissions, relative to controlled charging, across the country. Supplementary Figure A.42 [c] and [d] show that there is, however, a substantial reduction in cost and GHG benefits relative to unconstrained V2H. The average lifetime charging costs compared to a no-EV counterfactual increase from \$2.7k (5th and 95th percentile range: \$0.70–4.1k) to \$2.9k (\$0.88k–4.2k), and the average GHG emissions increase from -31tCO_2e (-53–5.9tCO_2e) to -5.7tCO_2e (-19–6.7tCO_2e). Note that this analysis is done for our base case objective function, which optimizes only for electricity cost. Results for an objective function which minimizes the sum of monetized GHG externalities and cost are in Supplementary Information Section A.4.1.

References

[1] O. Ouramdane, E. Elbouchikhi, Y. Amirat, F. Le Gall, and E. Sedgh Gooya, "Home Energy Management Considering Renewable Resources, Energy Storage, and an Electric Vehicle as a Backup," en, *Energies*, vol. 15, no. 8, p. 2830, Jan. 2022, Number: 8 Publisher: Multidisciplinary Digital Publishing Institute, ISSN: 1996-1073. DOI: 10.3390/en15082830. Accessed: Jul. 22, 2025. [Online]. Available: https://www.mdpi.com/1996-1073/15/8/2830 .

[2] B. Zafar and S. A. B. Slama, "PV-EV integrated home energy management using vehicle-to-home (V2H) technology and household occupant behaviors," *Energy Strategy Reviews*, vol. 44, p. 101 001, Nov. 2022, ISSN: 2211-467X. DOI: 10.1016/j.esr.2022.101001. Accessed: Jul. 22, 2025. [Online]. Available: https://www.sciencedirect.com/science/article/pii/S2211467X2200195X .

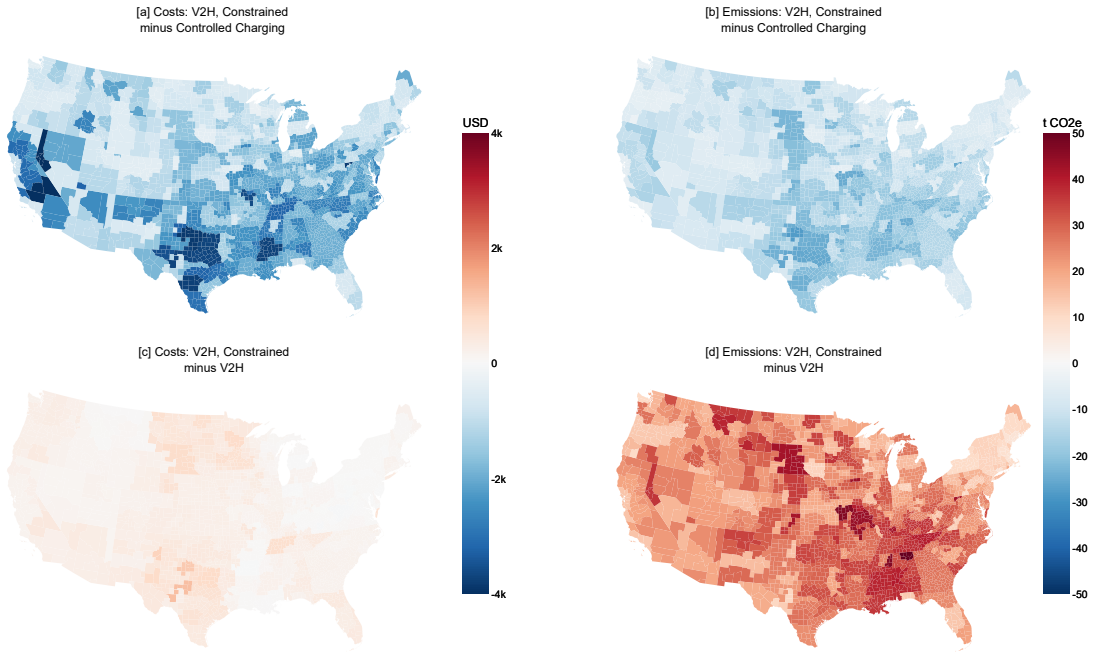


Figure A.42: **Effect of constraining V2H to 5kW and 5-9pm in order to reduce battery cycling with GHG externalities included in the objective function.** Change in lifetime median charging **a,** costs associated with shifting from controlled charging to constrained V2H, **b,** emissions associated with shifting from controlled charging to constrained V2H, **c,** costs associated with shifting from unconstrained V2H to constrained V2H, **d,** emissions associated with shifting from unconstrained V2H to constrained V2H. Results are labeled as "<Scenario 2> minus <Scenario 1>", where Scenario 1 represents a baseline (Controlled charging in [a] and [b] and unconstrained V2H in [c] [d]). Positive, red values indicate that going from Scenario 1 to 2 produces a worse outcome (more cost, emissions), while negative, blue values indicate an improvement (less cost, lower emissions). Results are for baseline homes. Compare with Figure 8, with results for the baseline case in which we optimize only for cost. Map GeoJSON from Plotly visualization tool[58].

[3] C. A. García-Vázquez, H. Espinoza-Ortega, F. Llorens-Iborra, and L. M. Fernández-Ramírez, "Feasibility analysis of a hybrid renewable energy system with vehicle-to-home operations for a house in off-grid and grid-connected applications," *Sustainable Cities and Society*, vol. 86, p. 104 124, 2022, Publisher: Elsevier.

[4] A. C. Duman, H. S. Erden, Ö. Gönül, and Ö. Güler, "A home energy management system with an integrated smart thermostat for demand response in smart grids," *Sustainable Cities and Society*, vol. 65, p. 102 639, 2021, Publisher: Elsevier.

[5] G. Azarbakhsh, A. Mahmoudi, S. Kahourzade, A. Yazdani, and A. Mahmud, "Optimal Sizing of Photovoltaic and Battery Energy Storage for Residential Houses in South Australia by Considering Vehicle-to-Home Operation," *IET renewable power generation*, vol. 19, no. 1, e70053, 2025, Publisher: Wiley Online Library.

[6] D. Kanakadhurga and N. Prabaharan, "Smart home energy management using demand response with uncertainty analysis of electric vehicle in the presence of renewable energy sources," *Applied Energy*, vol. 364, p. 123 062, 2024, Publisher: Elsevier.

[7] T. Higashitani, T. Ikegami, A. Uemichi, and A. Akisawa, "Evaluation of residential power supply by photovoltaics and electric vehicles," *Renewable Energy*, vol. 178, pp. 745–756, 2021, Publisher: Elsevier.

[8] D. M. Santos, P. Thüne, J. M. Zepter, and M. Marinelli, "Business cases for degradation-aware bidirectional charging of residential users and heavy-duty vehicle fleets," *eTransportation*, vol. 23, p. 100 389, 2025, Publisher: Elsevier.

[9] P. P. Patankar, Z. H. Rather, A. Nath, A. Liebman, and S. Doolla, "Vehicle-to-Home and Vehicle-to-Building: A Techno-Economic Analysis Under Varying Charging Methods and Tariff," *IEEE Transactions on Transportation Electrification*, 2024, Publisher: IEEE.

[10] J. Chen, J. Qing, and Q. Cai, "Impact of bi-directional electric vehicle and demand response on residential distributed PV capacity planning based on TOU pricing," *Journal of environmental management*, vol. 356, p. 120 689, 2024, Publisher: Elsevier.

[11] L. Pai, T. Senjyu, and M. H. Elkholy, "Integrated Home Energy Management with Hybrid Backup Storage and Vehicle-to-Home Systems for Enhanced Resilience, Efficiency, and Energy Independence in Green Buildings," en, *Applied Sciences*, vol. 14, no. 17, p. 7747, Jan. 2024, Number: 17 Publisher: Multidisciplinary Digital Publishing Institute, ISSN: 2076-3417. DOI: 10.3390/app14177747. Accessed: Jul. 22, 2025. [Online]. Available: https://www.mdpi.com/2076-3417/14/17/7747 .

[12] J. Niu, X. Li, Z. Tian, and H. Yang, "Uncertainty analysis of the electric vehicle potential for a household to enhance robustness in decision on the EV/V2H technologies," *Applied Energy*, vol. 365, p. 123 294, 2024, Publisher: Elsevier.

[13] M. Brennenstuhl, R. Otto, P. K. Elangovan, and U. Eicker, "The Potential of Vehicle-to-Home Integration for Residential Prosumers: A Case Study," en, *Smart Grids and Sustainable Energy*, vol. 9, no. 1, p. 25, May 2024, ISSN: 2731-8087. DOI: 10.1007/s40866-024-00206-4. Accessed: Jul. 22, 2025. [Online]. Available: https://doi.org/10.1007/s40866-024-00206-4 .

[14] J. Xu, J. Chen, H. Wei, Y. Zhao, B. Tian, Y. Wen, H. Jiang, N. Zhang, S. Zhang, and Y. Wu, "Emissions reduction potential and feasibility of vehicle-to-grid for Beijing' s future electric vehicles," English, *Cell Reports Physical Science*, vol. 0, no. 0, May 2025, Publisher: Elsevier, ISSN: 2666-3864. DOI: 10.1016/j.xcrp.2025.102616. Accessed: Jun. 6, 2025. [Online]. Available: https://www.cell.com/cell-reports-physical-science/abstract/S2666-3864(25)00215-2 .

[15] L. Franken, A. Hackett, J. Lizana, I. Riepin, R. Jenkinson, A. Lyden, L. Yu, and D. Friedrich, "Power system benefits of simultaneous domestic transport and heating demand flexibility in Great Britain' s energy transition," *Applied Energy*, vol. 377, p. 124 522, Jan. 2025, ISSN: 0306-2619. DOI: 10.1016/j.apenergy.2024.124522. Accessed: Jun. 6, 2025. [Online]. Available: https://www.sciencedirect.com/science/article/pii/S0306261924019056 .

[16] D. Borge-Diez, D. Icaza, E. Açıkkalp, and H. Amaris, "Combined vehicle to building (V2B) and vehicle to home (V2H) strategy to increase electric vehicle market share," *Energy*, vol. 237, p. 121 608, Dec. 2021, ISSN: 0360-5442. DOI: 10.1016/j.energy.2021.121608. Accessed: Jun. 6, 2025. [Online]. Available: https://www.sciencedirect.com/science/article/pii/S0360544221018569 .

[17] J. Chen, Y. Zhang, X. Li, B. Sun, Q. Liao, Y. Tao, and Z. Wang, "Strategic integration of vehicle-to-home system with home distributed photovoltaic power generation in Shanghai," *Applied Energy*, vol. 263, p. 114 603, Apr. 2020, ISSN: 0306-2619. DOI: 10.1016/j.apenergy.2020.114603. Accessed: Jun. 7, 2025. [Online]. Available: https://www.sciencedirect.com/science/article/pii/S030626192030115X .

[18] T. Gnann, S. Yu, J. Stute, and M. Kühnbach, "The value of smart charging at home and its impact on EV market shares –A German case study," *Applied Energy*, vol. 380, p. 124 997, Feb. 2025, ISSN: 0306-2619. DOI: 10.1016/j.apenergy.2024.124997. Accessed: Jun. 7, 2025. [Online]. Available: https://www.sciencedirect.com/science/article/pii/S030626192402381X .

[19] P. Vollmuth, D. Wohlschlager, L. Wasmeier, and T. Kern, "Prospects of electric vehicle V2G multi-use: Profitability and GHG emissions for use case combinations of smart and bidirectional charging today and 2030," *Applied Energy*, vol. 371, p. 123 679, Oct. 2024, ISSN: 0306-2619. DOI: 10.1016/j.apenergy.2024.123679. Accessed: Jun. 7, 2025. [Online]. Available: https://www.sciencedirect.com/science/article/pii/S0306261924010626 .

[20] Z. Zhong, W. Hu, and X. Zhao, "Rethinking electric vehicle smart charging and greenhouse gas emissions: Renewable energy growth, fuel switching, and efficiency improvement," *Applied Energy*, vol. 361, p. 122 904, May 2024, ISSN: 0306-2619. DOI: 10.1016/j.apenergy.2024.122904. Accessed: Jun. 7, 2025. [Online]. Available: https://www.sciencedirect.com/science/article/pii/S0306261924002873 .

[21] M. Singh, T. Yuksel, J. J. Michalek, and I. M. L. Azevedo, "Ensuring greenhouse gas reductions from electric vehicles compared to hybrid gasoline vehicles requires a cleaner U.S. electricity grid," en, *Scientific Reports*, vol. 14, no. 1, p. 1639, Jan. 2024, Publisher: Nature Publishing Group, ISSN: 2045-2322. DOI: 10.1038/s41598-024-51697-1. Accessed: Sep. 9, 2024. [Online]. Available: https://www.nature.com/articles/s41598-024-51697-1 .

[22] M. Bruchon, Z. L. Chen, and J. Michalek, "Cleaning up while Changing Gears: The Role of Battery Design, Fossil Fuel Power Plants, and Vehicle Policy for Reducing Emissions in the Transition to Electric Vehicles," *Environmental Science & Technology*, vol. 58, no. 8, pp. 3787–3799, Feb. 2024, ISSN: 0013-936X.

DOI: 10.1021/acs.est.3c07098. Accessed: May 8, 2024. [Online]. Available: https://doi.org/10.1021/acs.est.3c07098 .

[23] M. Tahir, S. Hu, and H. Zhu, "Strategic operation of electric vehicle in residential microgrid with vehicle-to-home features," *Energy*, vol. 308, p. 132 772, Nov. 2024, ISSN: 0360-5442. DOI: 10.1016/j.energy.2024.132772. Accessed: Jun. 5, 2025. [Online]. Available: https://www.sciencedirect.com/science/article/pii/S0360544224025465 .

[24] A. Jenn, "Emissions of electric vehicles in California' s transition to carbon neutrality," *Applied Energy*, vol. 339, p. 120 974, Jun. 2023, ISSN: 0306-2619. DOI: 10.1016/j.apenergy.2023.120974. Accessed: Mar. 20, 2024. [Online]. Available: https://www.sciencedirect.com/science/article/pii/S0306261923003380 .

[25] T. Kern, P. Dossow, and E. Morlock, "Revenue opportunities by integrating combined vehicle-to-home and vehicle-to-grid applications in smart homes," *Applied Energy*, vol. 307, p. 118 187, Feb. 2022, ISSN: 0306-2619. DOI: 10.1016/j.apenergy.2021.118187. Accessed: Feb. 13, 2025. [Online]. Available: https://www.sciencedirect.com/science/article/pii/S0306261921014586 .

[26] J. Owens, I. Miller, and E. Gençer, "Can vehicle-to-grid facilitate the transition to low carbon energy systems?" en, *Energy Advances*, vol. 1, no. 12, pp. 984–998, 2022. DOI: 10.1039/D2YA00204C. Accessed: Jun. 20, 2023. [Online]. Available: https://pubs.rsc.org/en/content/articlelanding/2022/ya/d2ya00204c .

[27] J. Chen, F. Wang, X. He, X. Liang, J. Huang, S. Zhang, and Y. Wu, "Emission mitigation potential from coordinated charging schemes for future private electric vehicles," en, *Applied Energy*, vol. 308, p. 118 385, Feb. 2022, ISSN: 0306-2619. DOI: 10.1016/j.apenergy.2021.118385. Accessed: Mar. 22, 2022. [Online]. Available: https://www.sciencedirect.com/science/article/pii/S0306261921016238 .

[28] S. P. Holland, M. J. Kotchen, E. T. Mansur, and A. J. Yates, "Why marginal CO2 emissions are not decreasing for US electricity: Estimates and implications for climate policy," *Proceedings of the National Academy of Sciences*, vol. 119, no. 8, e2116632119, Feb. 2022, Publisher: Proceedings of the National Academy of Sciences. DOI: 10.1073/pnas.2116632119. Accessed: Feb. 3, 2024. [Online]. Available: https://www.pnas.org/doi/abs/10.1073/pnas.2116632119 .

[29] Y. Tang, T. T. Cockerill, A. J. Pimm, and X. Yuan, "Reducing the life cycle environmental impact of electric vehicles through emissions-responsive charging," *iScience*, vol. 24, no. 12, p. 103 499, Dec. 2021, ISSN: 2589-0042. DOI: 10.1016/j.isci.2021.103499. Accessed: Jun. 5, 2025. [Online]. Available: https://www.sciencedirect.com/science/article/pii/S258900422101470X .

[30] C. R. Hung, S. Völler, M. Agez, G. Majeau-Bettez, and A. H. Strømman, "Regionalized climate footprints of battery electric vehicles in Europe," *Journal of Cleaner Production*, vol. 322, p. 129 052, Nov. 2021, ISSN: 0959-6526. DOI: 10.1016/j.jclepro.2021.129052. Accessed: Jun. 5, 2025. [Online]. Available: https://www.sciencedirect.com/science/article/pii/S0959652621032418 .

[31] C. Crozier, T. Morstyn, and M. McCulloch, "The opportunity for smart charging to mitigate the impact of electric vehicles on transmission and distribution systems," en, *Applied Energy*, vol. 268, p. 114 973, Jun. 2020, ISSN: 0306-2619. DOI: 10.1016/j.apenergy.2020.114973. Accessed: Jul. 14, 2021. [Online]. Available: https://www.sciencedirect.com/science/article/pii/S0306261920304852 .

[32] A. Jenn, "Emissions benefits of electric vehicles in Uber and Lyft ride-hailing services," en, *Nature Energy*, vol. 5, no. 7, pp. 520–525, Jul. 2020, Number: 7 Publisher: Nature Publishing Group, ISSN: 2058-7546. DOI: 10.1038/s41560-020-0632-7. Accessed: Sep. 21, 2022. [Online]. Available: https://www.nature.com/articles/s41560-020-0632-7 .

[33] N. B. G. Brinkel, W. L. Schram, T. A. AlSkaif, I. Lampropoulos, and W. G. J. H. M. van Sark, "Should we reinforce the grid? Cost and emission optimization of electric vehicle charging under different transformer limits," en, *Applied Energy*, vol. 276, p. 115 285, Oct. 2020, ISSN: 0306-2619. DOI: 10.1016/j.apenergy.2020.115285. Accessed: Oct. 13, 2020. [Online]. Available: http://www.sciencedirect.com/science/article/pii/S0306261920307972 .

[34] R. Tu, Y. (Gai, B. Farooq, D. Posen, and M. Hatzopoulou, "Electric vehicle charging optimization to minimize marginal greenhouse gas emissions from power generation," en, *Applied Energy*, vol. 277, p. 115 517, Nov. 2020, ISSN: 0306-2619. DOI: 10.1016/j.apenergy.2020.115517. Accessed: Oct. 4, 2020. [Online]. Available: http://www.sciencedirect.com/science/article/pii/S0306261920310291 .

[35] X. He, S. Zhang, Y. Wu, T. J. Wallington, X. Lu, M. A. Tamor, M. B. McElroy, K. M. Zhang, C. P. Nielsen, and J. Hao, "Economic and Climate Benefits of Electric Vehicles in China, the United States, and Germany," en, *Environmental Science & Technology*, vol. 53, no. 18, pp. 11 013–11 022, Sep. 2019, ISSN: 0013-936X, 1520-5851. DOI: 10.1021/acs.est.9b00531. Accessed: Jun. 8, 2021. [Online]. Available: https://pubs.acs.org/doi/10.1021/acs.est.9b00531 .

[36] X. Chen, H. Zhang, Z. Xu, C. P. Nielsen, M. B. McElroy, and J. Lv, "Impacts of fleet types and charging modes for electric vehicles on emissions under different penetrations of wind power," *Nature Energy*, vol. 3, no. 5, pp. 413–421, 2018, Publisher: Nature Publishing Group.

[37] A. Weis, P. Jaramillo, and J. Michalek, "Consequential life cycle air emissions externalities for plug-in electric vehicles in the PJM interconnection," en, *Environmental Research Letters*, vol. 11, no. 2, p. 024 009, Feb. 2016, Publisher: IOP Publishing, ISSN: 1748-9326. DOI: 10.1088/1748-9326/11/2/024009. Accessed: Apr. 25, 2024. [Online]. Available: https://dx.doi.org/10.1088/1748-9326/11/2/024009 .

[38] A. C. Duman, H. S. Erden, Ö. Gönül, and Ö. Güler, "Optimal sizing of PV-BESS units for home energy management system-equipped households considering day-ahead load scheduling for demand response and self-consumption," *Energy and Buildings*, vol. 267, p. 112 164, 2022, Publisher: Elsevier.

[39] Meteostat, *The Weather's Record Keeper*, en, 2024. Accessed: Jul. 20, 2024. [Online]. Available: https://meteostat.net/en/ .

[40] L. Vimmerstedt, T. Stehly, S. Akar, A. Sekar, B. Mirletz, D. Stright, C. Augustine, P. Beiter, P. Bhaskar, N. Blair, S. Cohen, W. Cole, P. Duffy, D. Feldman, P. Gagnon, P. Kurup, C. Murphy, V. Ramasamy, J. Robins, J. Zuboy, D. Oladosu, and J. Hoffmann, "2022 Annual Technology Baseline (ATB) Cost and Performance Data for Electricity Generation Technologies," English, DOE Open Energy Data Initiative (OEDI); National Renewable Energy Laboratory (NREL), Tech. Rep. 5716, Jun. 2022. DOI: 10.25984/1871952. Accessed: Jul. 23, 2023. [Online]. Available: https://www.osti.gov/dataexplorer/biblio/dataset/1871952 .

[41] "Annual Energy Outlook 2023," U.S. Energy Information Administration, Tech. Rep., 2023. [Online]. Available: https://www.eia.gov/outlooks/aeo/ .

[42] N. Ireson, *The 25 Most Popular SUVs in 2024*, en-US, Publication Title: Kelley Blue Book, Jan. 2025. Accessed: Mar. 15, 2025. [Online]. Available: https://www.kbb.com/best-cars/most-popular-suvs/ .

[43] U.S. DOE, *2024 Honda CR-V FWD*, 2024. Accessed: Mar. 15, 2025. [Online]. Available: https://www.fueleconomy.gov/feg/Find.do?action=sbs&id=46694 .

[44] D. Wu, F. Guo, F. R. I. Field, R. D. De Kleine, H. C. Kim, T. J. Wallington, and R. E. Kirchain, "Regional Heterogeneity in the Emissions Benefits of Electrified and Lightweighted Light-Duty Vehicles," *Environmental Science & Technology*, vol. 53, no. 18, pp. 10 560–10 570, Sep. 2019, Publisher: American Chemical Society, ISSN: 0013-936X. DOI: 10.1021/acs.est.9b00648. Accessed: Sep. 5, 2023. [Online]. Available: https://doi.org/10.1021/acs.est.9b00648 .

[45] M. Wang et al., *Greenhouse gases, Regulated Emissions, and Energy use in Technologies Model ® (2023 Excel)*, Language: en, 2023. DOI: 10.11578/GREET-EXCEL-2023/DC.20230907.1. Accessed: Oct. 4, 2024. [Online]. Available: https://www.osti.gov/doecode/biblio/113174 .

[46] *U.S. Regular All Formulations Retail Gasoline Prices (Dollars per Gallon)*. Accessed: Jul. 3, 2025. [Online]. Available: https://www.eia.gov/dnav/pet/hist/leafhandler.ashx?n=pet&s=emm_epmr_pte_nus_dpg&f=m .

[47] S. Bhoir, P. Caliandro, and C. Brivio, "Impact of V2G service provision on battery life," *Journal of Energy Storage*, vol. 44, p. 103 178, 2021, Publisher: Elsevier. Accessed: Jul. 20, 2024. [Online]. Available: https://www.sciencedirect.com/science/article/pii/S2352152X21008781?casa_token=bmUybBp3_NQAAAAA:3v-t13TvYJCOZ7hjynp4RgM3CM9td6nYi-gSzOT_M8TwwdtIsaGo6hnsmNG2hCL_BsnL_W46 .

[48] J. Guo, J. Yang, Z. Lin, C. Serrano, and A. M. Cortes, "Impact analysis of v2g services on ev battery degradation-a review," *2019 IEEE Milan PowerTech*, pp. 1–6, 2019, Publisher: IEEE. Accessed: Jul. 20, 2024. [Online]. Available: https://ieeexplore.ieee.org/abstract/document/8810982/ .

[49] O. Kolawole and I. Al-Anbagi, "The impact of EV battery cycle life on charge-discharge optimization in a V2G environment," in *2018 IEEE Power & Energy Society Innovative Smart Grid Technologies Conference (ISGT)*, IEEE, 2018, pp. 1–5. Accessed: Jul. 20, 2024. [Online]. Available: https://ieeexplore.ieee.org/abstract/document/8403393/?casa_token=qP4kQnouVpwAAAAA:YekpnD_DZBvGhyF0M27kGTkxH2UlZnWap6vic07uAzRrX6ZaHhdmC6T_EBKq40NRJlmG-tXtNw .

[50] P. Gasper, A. Saxon, Y. Shi, E. Endler, K. Smith, and F. M. Thakkar, "Degradation and modeling of large-format commercial lithium-ion cells as a function of chemistry, design, and aging conditions," *Journal of Energy Storage*, vol. 73, p. 109 042, Dec. 2023, ISSN: 2352-152X. DOI: 10.1016/j.est.2023.109042. Accessed: Sep. 9, 2024. [Online]. Available: https://www.sciencedirect.com/science/article/pii/S2352152X23024404 .

[51] A. Leippi, M. Fleschutz, K. Davis, A.-L. Klingler, and M. D. Murphy, "Optimizing electric vehicle fleet integration in industrial demand response: Maximizing vehicle-to-grid benefits while compensating vehicle owners for battery degradation," *Applied Energy*, vol. 374, p. 123 995, Nov. 2024, ISSN: 0306-2619. DOI: 10.1016/j.apenergy.2024.123995. Accessed: Oct. 22, 2024. [Online]. Available: https://www.sciencedirect.com/science/article/pii/S0306261924013783 .

[52] J. Schmalstieg, S. Käbitz, M. Ecker, and D. U. Sauer, "A holistic aging model for Li(NiMnCo)O2 based 18650 lithium-ion batteries," *Journal of Power Sources*, vol. 257, pp. 325–334, Jul. 2014, ISSN: 0378-7753. DOI: 10.1016/j.jpowsour.2014.02.012. Accessed: Apr. 30, 2024. [Online]. Available: https://www.sciencedirect.com/science/article/pii/S0378775314001876 .

[53] J. Gong, D. Wasylowski, J. Figgener, S. Bihn, F. Rücker, F. Ringbeck, and D. U. Sauer, "Quantifying the impact of V2X operation on electric vehicle battery degradation: An experimental evaluation," *eTransportation*, vol. 20, p. 100 316, May 2024, ISSN: 2590-1168. DOI: 10.1016/j.etran.2024.100316. Accessed: Oct. 22, 2024. [Online]. Available: https://www.sciencedirect.com/science/article/pii/S2590116824000067 .

[54] D. Wohlschlager, S. Kigle, V. Schindler, A. Neitz-Regett, and M. Fröhling, "Environmental effects of vehicle-to-grid charging in future energy systems –A prospective life cycle assessment," *Applied Energy*, vol. 370, p. 123 618, Sep. 2024, ISSN: 0306-2619. DOI: 10.1016/j.apenergy.2024.123618. Accessed: Oct. 22, 2024. [Online]. Available: https://www.sciencedirect.com/science/article/pii/S0306261924010018 .

[55] M. Naumann, "Techno-economic evaluation of stationary battery energy storage systems with special consideration of aging," Ph.D. dissertation, Technische Universität München, 2018. Accessed: Jun. 27, 2024. [Online]. Available: https://mediatum.ub.tum.de/1434981 .

[56] L. Wildfeuer, A. Karger, D. Aygül, N. Wassiliadis, A. Jossen, and M. Lienkamp, "Experimental degradation study of a commercial lithium-ion battery," *Journal of Power Sources*, vol. 560, p. 232 498, Mar. 2023, ISSN: 0378-7753. DOI: 10.1016/j.jpowsour.2022.232498. Accessed: May 2, 2024. [Online]. Available: https://www.sciencedirect.com/science/article/pii/S0378775322014756 .

[57] J. Schneider, O. Teichert, M. Zähringer, K. Götz, and M. Lienkamp, "Spoilt for Choice: User-Centric Choice of Battery Size and Chemistry for Battery-Electric Long-Haul Trucks," en, *Energies*, vol. 17, no. 1, p. 158, Jan. 2024, Number: 1 Publisher: Multidisciplinary Digital Publishing Institute, ISSN: 1996-1073. DOI: 10.3390/en17010158. Accessed: Nov. 23, 2024. [Online]. Available: https://www.mdpi.com/1996-1073/17/1/158 .

[58] Plotly, *Plotly Datasets*, 2025. [Online]. Available: https://raw.githubusercontent.com/plotly/datasets/master/geojson-counties-fips.json .

[59] A. D. Mills, T. Levin, R. Wiser, J. Seel, and A. Botterud, "Impacts of variable renewable energy on wholesale markets and generating assets in the United States: A review of expectations and evidence," en, *Renewable and Sustainable Energy Reviews*, vol. 120, p. 109 670, Mar. 2020, ISSN: 1364-0321. DOI: 10.1016/j.rser.2019.109670. Accessed: Jul. 1, 2023. [Online]. Available: https://www.sciencedirect.com/science/article/pii/S1364032119308755 .

[60] S. Sagaria, M. van der Kam, and T. Boström, "Vehicle-to-grid impact on battery degradation and estimation of V2G economic compensation," *Applied Energy*, vol. 377, p. 124 546, Jan. 2025, ISSN: 0306-2619. DOI: 10.1016/j.apenergy.2024.124546. Accessed: Oct. 22, 2024. [Online]. Available: https://www.sciencedirect.com/science/article/pii/S0306261924019299 .

APPENDIX B

Supplementary Information for 'Negative Electric Vehicle Emissions: Vehicle-to-Grid Can Incentivize Enough Wind and Solar Investment to Reverse EV Charging Emissions'

B.1 Supplementary Literature Review

This section provides supplementary literature review to the main body (Table 4.1). Current studies assess emission impacts of plug-in electric vehicle adoption and charging interventions mainly with two approaches, focusing either on the power system operation

or on the power system capacity expansion. The first approach assesses emission impacts induced by grid intervention with a fixed power system[1], [2], [3], [4], [5], [6]. Tu et al. 2020 and Holland et al. 2022 used marginal emission factors to evaluate emission impacts of PEV charging intervention.[1], [2] Chen et al. 2018 used a power system dispatch model to assess the emission impacts of charging intervention in fixed power systems [7]. However, Owens et al. and Gagnon et al. [8], [9] note that, in the long run, grid interventions like EV adoption can induce changes in the trajectory of power system generator capacity expansion, and this structural change of the power system also has climate implications.

Other relevant studies employ capacity expansion models (CEMs). However, CEMs typically do not model granular short-term power system constraints, and many of these studies make simplification assumptions about grid operation [8], [10], [11]. Brown et al. 2018 assessed cost reduction effects of grid flexibility options provided by the building sector and the transportation sector [10]. Though their model included PEV with smart charging and V2G, it represented PEV flexibility with stationary storage of 50% capacity of PEVs. This simplification can be necessary for CEMs but lacks representation of operational constraints that are vital to understanding PEV flexibility. Weis et al. 2014 managed to join the force of an operational cost model and a capacity expansion model[12]. The study ran power system simulation for 4 representative weeks of a year and used the results as inputs for a capacity expansion model. As a result, the study's scalability was limited. Moreover, the study did not model V2G. Owens et al. 2022, based on a CEM, represented V2G operation in the model with detailed operational constraints, informed by real-world travel records [8]. However, they only allow V2G to participate in the ancillary service market but not in the energy market, which limits the potential of V2G. Moreover, the study only considers a hypothetical optimal power system that is built from scratch and does not consider effects of installed fossil fuel generators on grid interventions, which, can increase system emissions with large scale deployment of energy storage and[13] While the investigation done by existing studies have been insightful and fruitful, a holistic view that combines power system

operation and capacity expansion helps answer the question better, as it is the short-term operational constraints that ultimately determines the system operation outcome.

Furthermore, by ignoring transmission constraints between grid regions, along with the possibility that generation and EV loads are added in different regions, the study omits probable spatial mismatch between V2G and generation. As for the spatial nuances, V2G service is best available in load centers [14], [15], whereas much of variable renewable energy generation capacity is located in distant and rural areas [16], [17]. This mismatch of the spatial distribution of demand and supply also affects the value of grid flexibility options such as flexible PEV load.

Table B.1. Comparison of method and materials of existing studies and this study. VRE is short for variable renewable energy.

Author and year	Modeling of operational constraints of grid intervention	Realistic BEV charging profiles	Endogenous capacity expansion	Consideration of existing fossil fuel generators	Analysis of impacts of grid intervention on VRE deployment	Endogenous power system operation modeling	V2G modeling
Owens et al. 2022 [8]	✓		✓		✓	✓	✓
Holland et al. 2022 [1]				✓			
Gagnon & Cole 2022 [9]			✓	✓	✓	✓	
Carrión et al. 2015 [18]	✓		✓	✓	✓		
Shi et al. 2020 [5]	✓			✓		✓	✓
Manríquez et al. 2020 [11]	✓			✓		✓	✓
Jenn et al. 2020 [19]		✓	✓	✓		✓	
Weis et al. 2014 [12]	✓	✓	✓		✓	✓	
Weis et al. 2015 [20]	✓	✓		✓	✓	✓	
Nunes & Brito 2017 [21]	✓	✓				✓	✓
Forrest et al. 2016 [22]	✓	✓		✓		✓	✓
Tarroja et al. 2016 [23]	✓	✓				✓	✓
This study	✓	✓	✓	✓	✓	✓	✓

B.2 Sensitivity analysis

B.2.1 Higher stationary storage

In the base case, the PJM power system has 5.4 GW(42 GWh) grid-scale storage units. The assumed stationary storage is constant against varying wind and solar power penetration levels. To test the robustness of our results against the addition of more stationary storage capacity, we run the analysis with more battery storage capacity, where the total stationary storage capacity is increased to 14 GW (56 GWh).

Shown in Figure B.1, V2G increases the maximum profitable capacity of wind and solar capacity by 4.2 GW (a 6% increase), significantly lower than under the base case: 15 GW (from 64 GW to 79 GW, a 23% increase). As the system's demand for grid flexibility is saturated by the addition of stationary storage, benefits provided by V2G significantly diminish.

As a result of lower induced wind and solar capacity investment, the wind and solar generation changes induced by V2G under the high battery scenario are also smaller than the base case (shown in Figure B.2). When induced capacity investment is considered, wind and solar generation increases (15 TWh) are much lower than under the base case (45 TWh).

Due to changes of generation mix, total system costs differ under different charging scenarios. When ignoring induced wind and solar capacity investment, total system costs under V2G are 0.20% higher than without PEVs ($13 per PEV per year increase). When accounting for induced wind and solar capacity investment, total system costs under V2G are 3% lower than without PEVs ($180 per PEV per year reduction). System cost reduction per PEV per year is 80% lower than the base case.

As a result of changes discussed above, V2G's emission externality reduction benefits are also significantly diminished (see Figure B.3). When considering induced wind and solar capacity investment, V2G reduces air emission externalities by $630 per PEV, compared

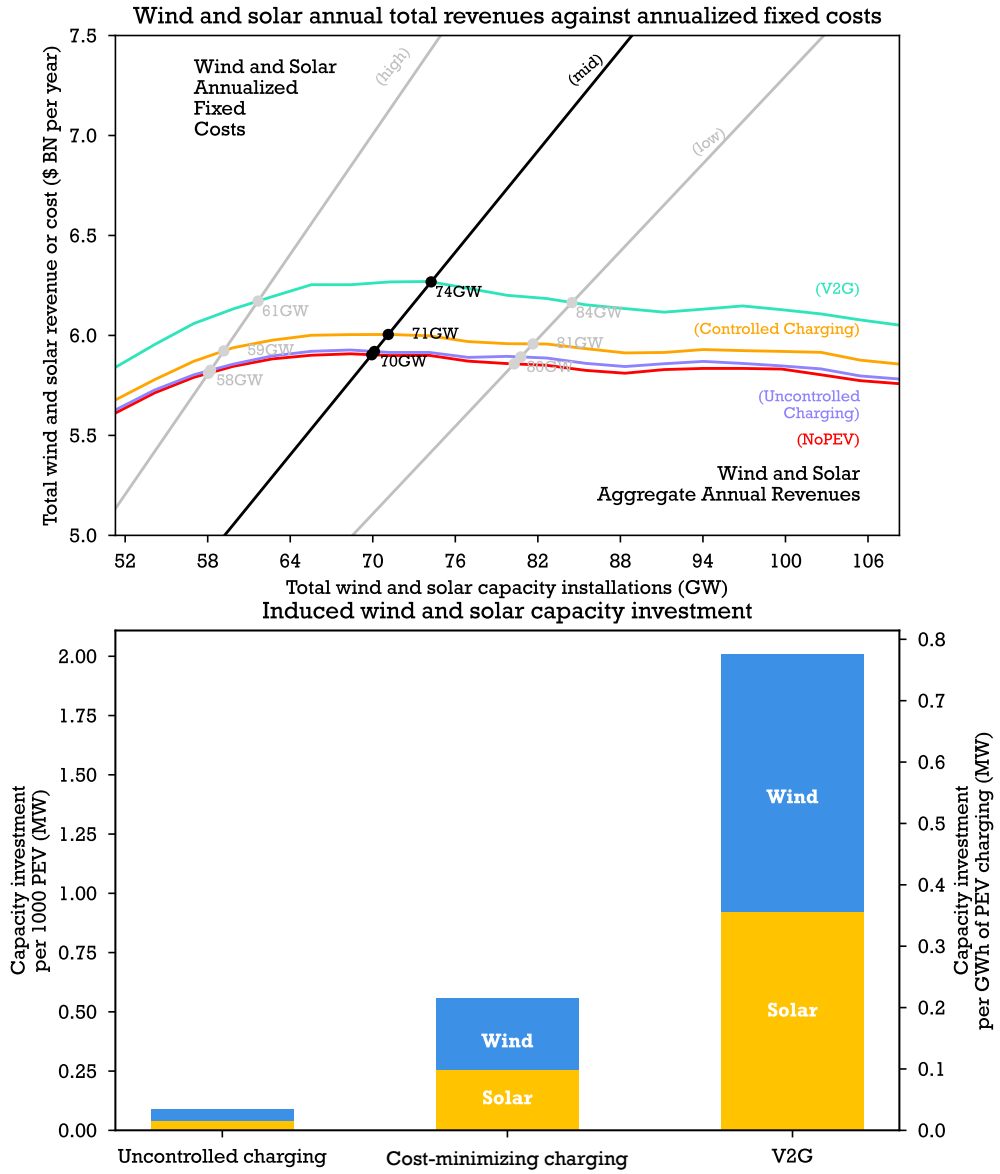


Figure B.1: Effect of PEV charging load on the economics of wind and solar capacity investment. Top panel: Total revenues and total annualized fixed costs for solar and wind generators, by PEV and PEV charging intervention scenarios and by wind and solar fixed cost scenarios. **All results in this figure are run with additional stationary storage than the base case (14 GW compared with 5.4 GW).** All other parameters are the same. Note: (high): conservative fixed cost scenario, (mid): base case fixed cost scenario, (low): optimistic fixed cost scenario. Bottom panel: Wind and solar capacity investment induced by PEV charging interventions, including uncontrolled charging (UC), cost-minimizing charging (CC) and vehicle-to-grid (V2G), relative to the NoPEV baseline scenario. The currency unit is 2024 USD. $ BN is short for billion USD. Further detailed methods are described in the method section.

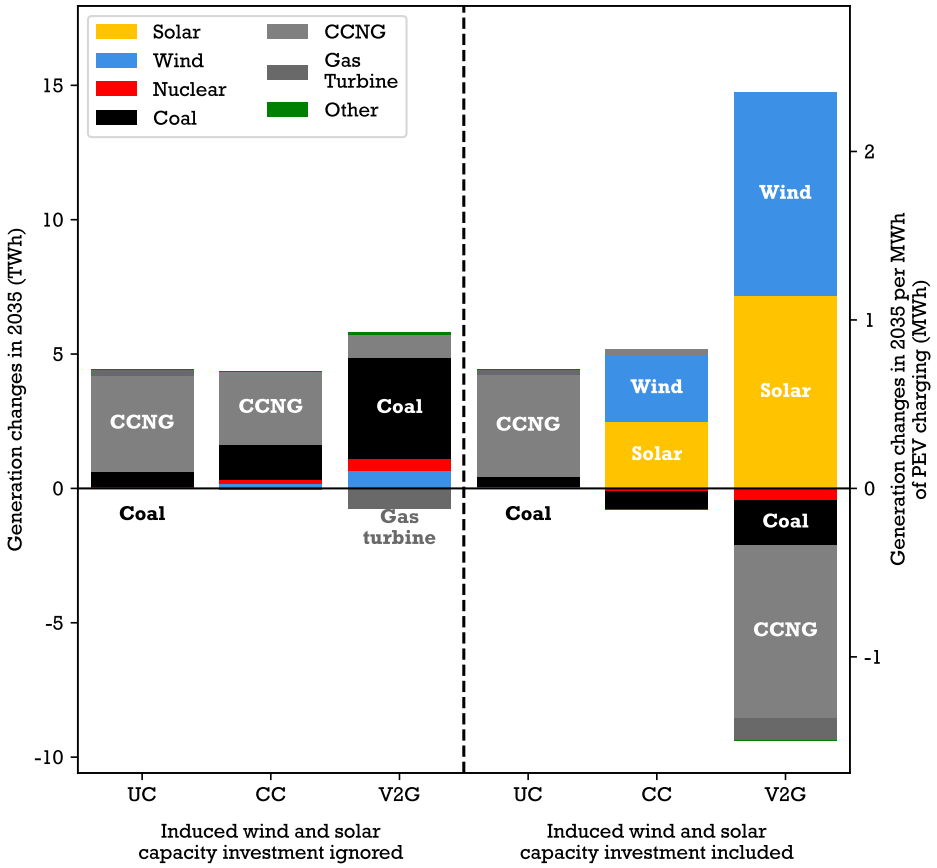


Figure B.2: Effect of PEV charging load on power generation. Changes in annual generation by fuel type, relative to the NoPEV case, for each PEV charging scenario when ignoring versus including induced wind and solar capacity investment. **All results in this figure are run with additional stationary storage than the base case (14 GW compared with 5.4 GW in the base case).** All other parameters are the same. 'CCNG' fuel type includes combined cycle natural gas generators. 'Other' fuel types include biomass, fossil waste, fuel cell, hydro, landfill gas, municipal solid waste, non-fossil waste, and oil or gas steam.

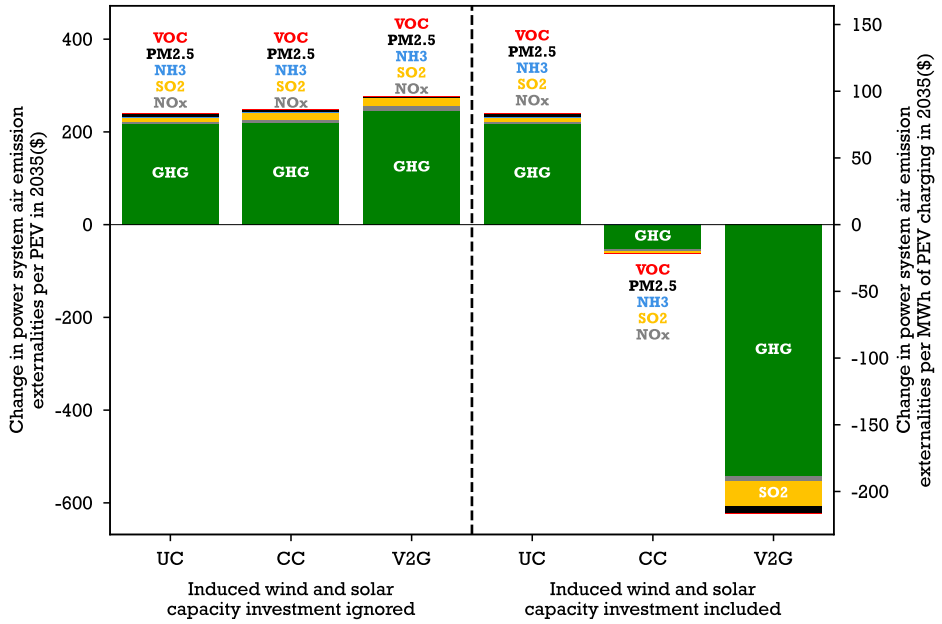


Figure B.3: Effect of PEV charging on power system air emission externalities. Change in total power system air emission externalities per PEV and per MWh of PEV charging in 2035, relative to the NoPEV scenario, under each PEV charging scenario when ignoring versus including induced wind and solar capacity investment. **All results in this figure are run with additional stationary storage than the base case (14 GW compared with 5.4 GW in the base case).** The 'ignored' scenarios use generation portfolios given by PJM's grid planning study for 2035 [24]. The 'included' scenarios consider wind and solar capacity at maximum profitable capacity, as described in Method and Materials.

with $2200 under the base case.

B.2.2 Higher transmission

To test the robustness of our results against the addition of more transmission capacity, we run the analysis with double the transmission capacity compared to the base case.

Shown in Figure B.4, V2G increases the maximum profitable capacity of wind and solar capacity by 20 GW (from 71 GW to 91 GW, a 28% increase), higher than under the base case: 15 GW (from 64 GW to 79 GW, a 23% increase). V2G benefits from better interconnectedness with the transmission capacity expansion.

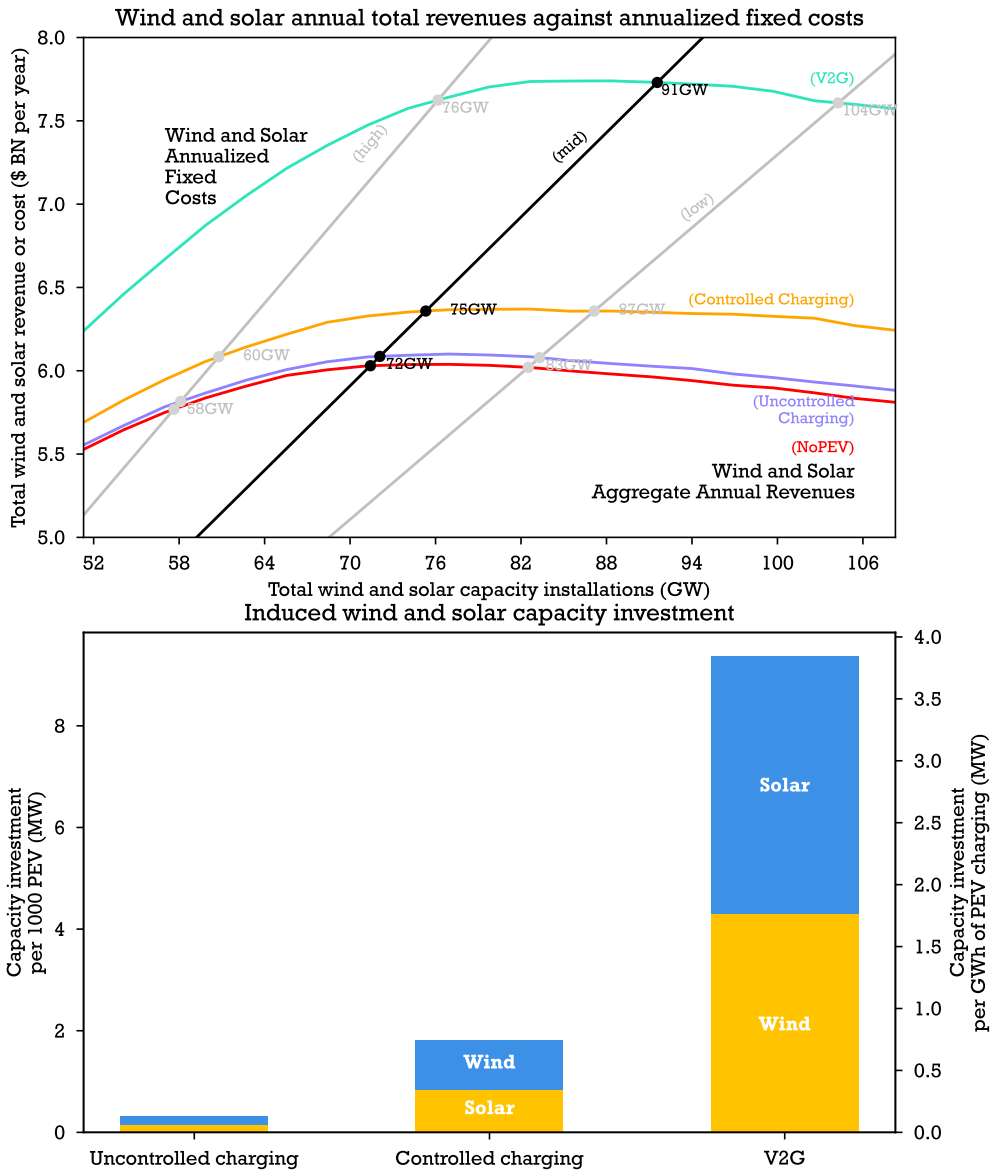


Figure B.4: Effect of PEV charging load on the economics of wind and solar capacity investment. Top panel: Total revenues and total annualized fixed costs for solar and wind generators, by PEV and PEV charging intervention scenarios and by wind and solar fixed cost scenarios. **All results in this figure are run with twice as much transmission capacity as the base case.** All other parameters are the same. Note: (high): conservative fixed cost scenario, (mid): base case fixed cost scenario, (low): optimistic fixed cost scenario. Bottom panel: Wind and solar capacity investment induced by PEV charging interventions, including uncontrolled charging (UC), cost-minimizing charging (CC) and vehicle-to-grid (V2G), relative to the NoPEV baseline scenario. The currency unit is 2024 USD. $ BN is short for billion USD. Further detailed methods are described in the method section.

As a result of more induced wind and solar capacity investment, the wind and solar generation changes induced by V2G under the high transmission scenario are also larger than the base case (shown in Figure B.5). When induced capacity investment is considered, wind and solar generation increases (55 TWh) are 22% higher than under the base case (45 TWh).

When ignoring induced wind and solar capacity investment, total system costs under V2G are 5.2% lower than without PEVs ($340 per PEV per year reduction). When accounting for induced wind and solar capacity investment, total system costs under V2G are 18% lower than without PEVs ($1100 per PEV per year reduction). System cost reduction per PEV per year is 25% higher than the base case.

As a result of changes discussed above, V2G reduces air emission externalities by $2900 per PEV, 32% higher compared with $2200 under the base case (see Figure B.6).

B.2.3 Higher PEV penetration

In the base case, we assume the PEV fleet accounts for 10% of PJM's light-duty passenger vehicles. To test the robustness of our results with more PEVs in the system, we run the analysis with more PEVs, where the number of PEVs is doubled.

Shown in Figure B.7, with a larger PEV fleet, the total wind and solar capacity investment induced by V2G increases significantly. Under a high PEV penetration scenario, V2G increases the maximum profitable capacity of wind and solar capacity by 24 GW (a 39% increase) for a combined wind and solar capacity of 64 GW with no PEVs. The increases are 60% higher than under the base case: 15 GW (a 23% increase) increase for a combined capacity with no PEVs of 64 GW. On the per GWh charging demand basis, however, the induced capacity investments with higher PEV penetration (2.3 MW/GWh of PEV charging) are lower than the base case (2.9 MW/GWh of PEV charging). The capacity investment induction benefits of V2G are only diluted by 20% despite doubling the number of PEVs.

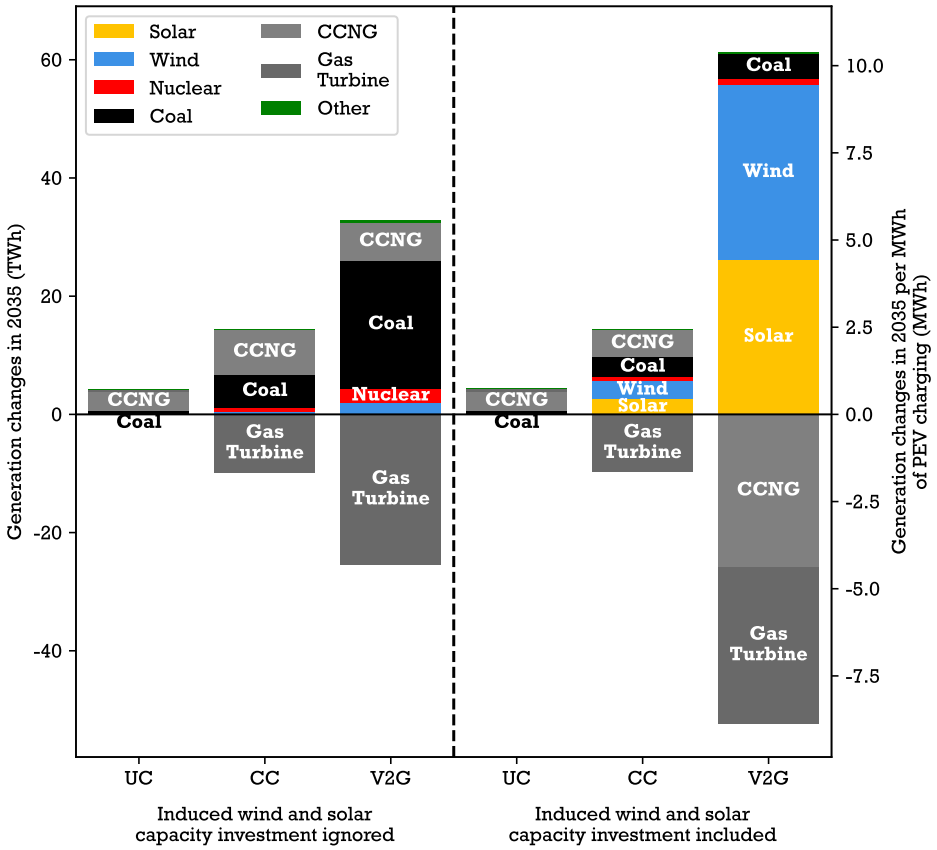


Figure B.5: Effect of PEV charging load on power generation. Changes in annual generation by fuel type, relative to the NoPEV case, for each PEV charging scenario when ignoring versus including induced wind and solar capacity investment. **All results in this figure are run with twice as much transmission capacity as the base case.** All other parameters are the same. 'CCNG' fuel type includes combined cycle natural gas generators. 'Other' fuel types include biomass, fossil waste, fuel cell, hydro, landfill gas, municipal solid waste, non-fossil waste, and oil or gas steam.

As a result of higher induced wind and solar capacity investment, the wind and solar generation changes induced by V2G under the high battery scenario are also higher than the base case (shown in Figure B.8). When induced capacity investment is considered, wind and solar generation increases (68 TWh) are 51% higher than under the base case (45 TWh). On the per MWh of PEV charging basis, wind and solar generation increases by 5.8 MWh for every MWh of PEV charging, compared with 7.8 MWh under the base case. The wind and solar generation increase is diluted by 26% due to the addition of PEVs to the system.

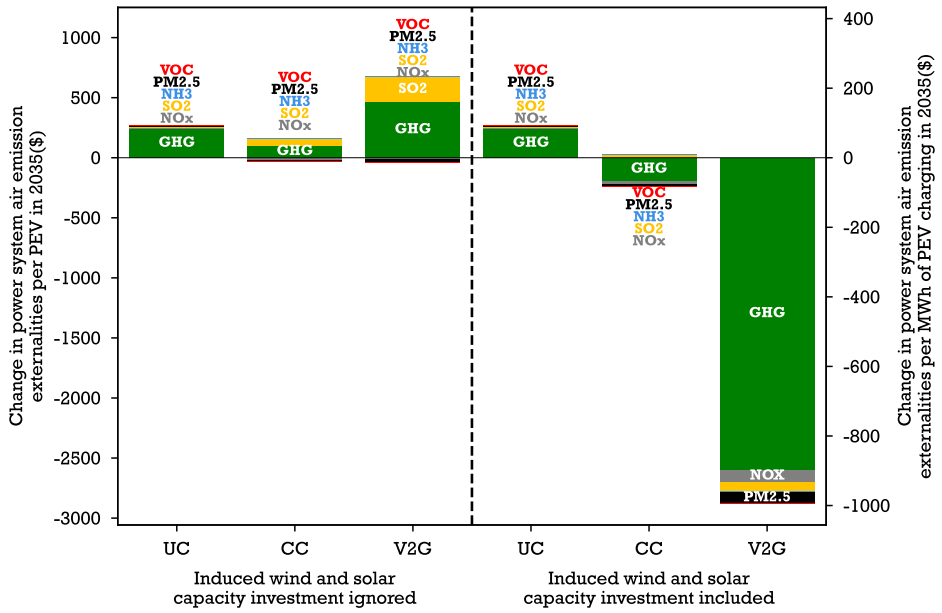


Figure B.6: Effect of PEV charging on power system air emission externalities. Change in total power system air emission externalities per PEV and per MWh of PEV charging in 2035, relative to the NoPEV scenario, under each PEV charging scenario when ignoring versus including induced wind and solar capacity investment. **All results in this figure are run with twice as much transmission capacity as the base case.** The 'ignored' scenarios use generation portfolios given by PJM's grid planning study for 2035 [24]. The 'included' scenarios consider wind and solar capacity at maximum profitable capacity, as described in Method and Materials.

When ignoring induced wind and solar capacity investment, total system costs under V2G are 5.2% lower than without PEVs ($170 per PEV per year reduction). When accounting for induced wind and solar capacity investment, total system costs under V2G are 19% lower than without PEVs ($620 per PEV per year reduction).

As a result of higher wind and solar installed capacity and generation discussed above, doubling the number of PEVs also increases V2G's air emission externality reduction benefits (shown in Figure B.9). With a PEV penetration of 20%, total air emission externalities are reduced by $1500 per PEV per year, 32% less compared with the base case. Though doubling the number of PEVs dilutes emission externality reduction on the per PEV basis, the benefit dilution lags behind the penetration increase.

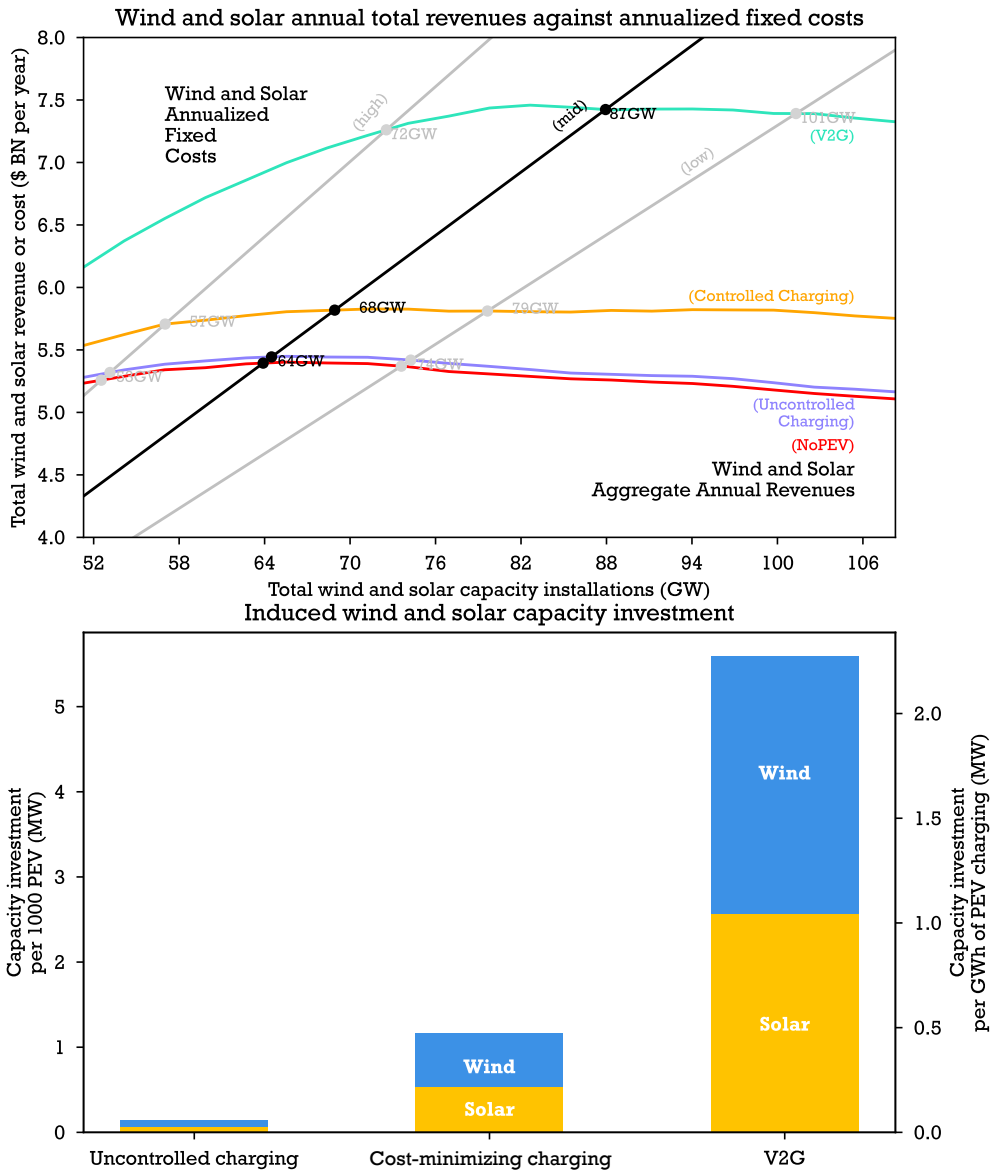


Figure B.7: Effect of PEV charging load on the economics of wind and solar capacity investment. Top panel: Total revenues and total annualized fixed costs for solar and wind generators, by PEV and PEV charging intervention scenarios and by wind and solar fixed cost scenarios. **All results in this figure are run with 20% PEV penetration.** All other parameters are the same. Note: (high): conservative fixed cost scenario, (mid): base case fixed cost scenario, (low): optimistic fixed cost scenario. Bottom panel: Wind and solar capacity investment induced by PEV charging interventions, including uncontrolled charging (UC), cost-minimizing charging (CC) and vehicle-to-grid (V2G), relative to the NoPEV baseline scenario. The currency unit is 2024 USD. $ BN is short for billion USD. Further detailed methods are described in the method section.

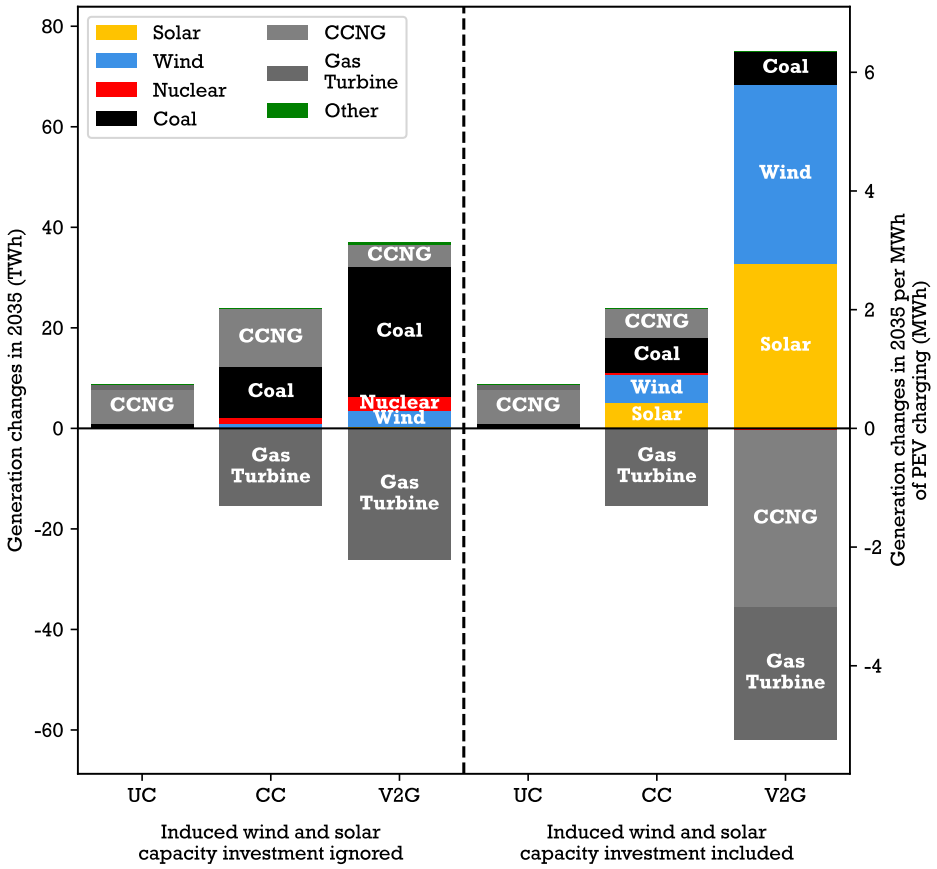


Figure B.8: Effect of PEV charging load on power generation. Changes in annual generation by fuel type, relative to the NoPEV case, for each PEV charging scenario when ignoring versus including induced wind and solar capacity investment. **All results in this figure are run with 20% PEV penetration.** All other parameters are the same. When accounting for induced wind and solar investment, wind and solar capacity and therefore generation vary across PEV charging scenarios. 'CCNG' fuel type includes combined cycle natural gas generators. 'Other' fuel types include biomass, fossil waste, fuel cell, hydro, landfill gas, municipal solid waste, non-fossil waste, and oil or gas steam.

B.2.4 Wind and solar capacity buildouts

To test the sensitivity of our results on the assumed fixed wind-to-solar capacity ratio, we run a high solar scenario, where solar capacity is increased by 10% and wind reduced by 10% compared with the base case, and a high wind scenario, where wind capacity is increased by 10% and solar reduced by 10% compared with the base case. The comparison with base case shows that while results are sensitive to wind and solar generation profiles, the conclusion still stands that PEVs under V2G can induce wind

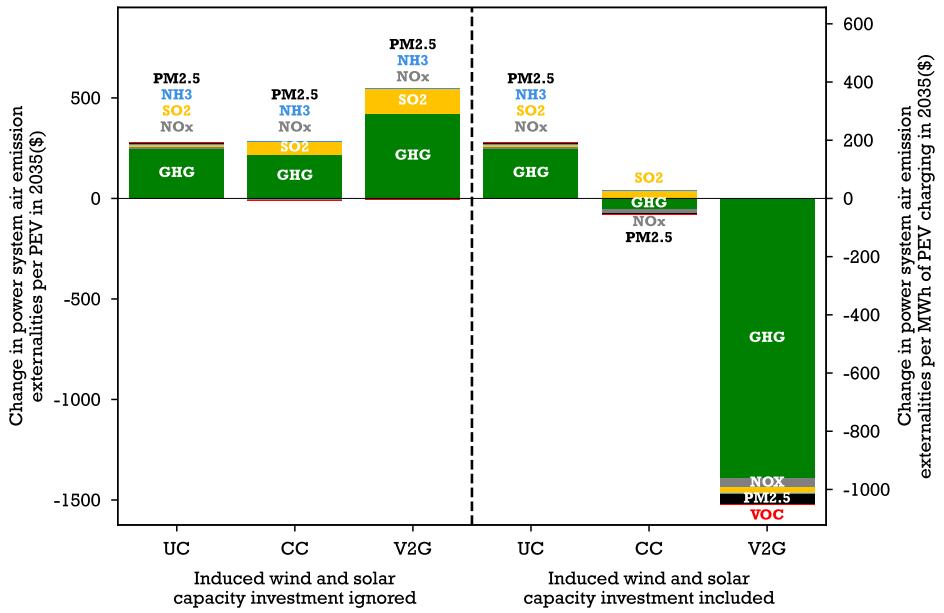


Figure B.9: Effect of PEV charging on power system air emission externalities. Change in total power system air emission externalities per PEV and per MWh of PEV charging in 2035, relative to the NoPEV scenario, under each PEV charging scenario when ignoring versus including induced wind and solar capacity investment. The 'ignored' scenarios use generation portfolios given by PJM's grid planning study for 2035 [24]. The 'included' scenarios consider wind and solar capacity at maximum profitable capacity, as described in Method and Materials. **All results in this figure are run with 20% PEV penetration.** All other parameters are the same.

and solar capacity expansion, reduce overall power grid system costs and overall power grid emission externalities despite PEV charging.

B.2.4.1 High solar scenario

Shown in Figure B.10, with more solar and less wind, the total wind and solar capacity investment induced by V2G changes notably, but capacity investment induction benefits persists and are even higher than the base case. Under a high solar scenario, V2G increases the maximum profitable capacity of wind and solar capacity by 18 GW (a 26% increase) for a combined wind and solar capacity of 70 GW with no PEVs. The increases are 20% higher than under the base case: 15 GW (a 23% increase) increase for a combined capacity with no PEVs of 64 GW.

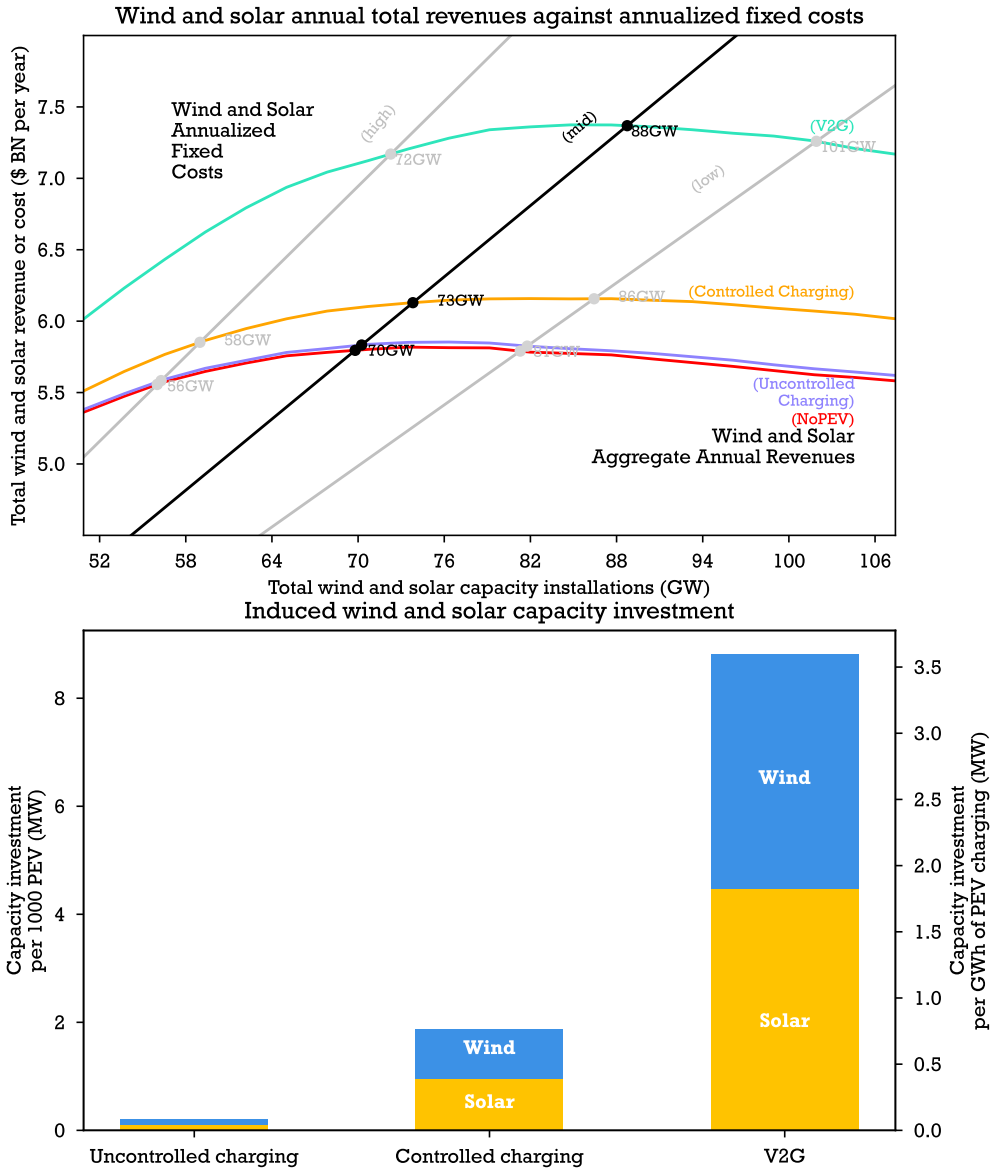


Figure B.10: Effect of PEV charging load on the economics of wind and solar capacity investment. Top panel: Total revenues and total annualized fixed costs for solar and wind generators, by PEV and PEV charging intervention scenarios and by wind and solar fixed cost scenarios. **All results in this figure are run with additional solar capacity and lower wind capacity.** All other parameters are the same. Note: (high): conservative fixed cost scenario, (mid): base case fixed cost scenario, (low): optimistic fixed cost scenario. Bottom panel: Wind and solar capacity investment induced by PEV charging interventions, including uncontrolled charging (UC), cost-minimizing charging (CC) and vehicle-to-grid (V2G), relative to the NoPEV baseline scenario. The currency unit is 2024 USD. $ BN is short for billion USD. Further detailed methods are described in the method section.

As a result of higher induced wind and solar capacity investment, the wind and solar generation changes induced by V2G under the high battery scenario are also higher than in the base case (shown in Figure B.11). When induced capacity investment is considered, wind and solar generation increases (60 TWh) are 25% higher than under the base case (45 TWh).

When ignoring induced wind and solar capacity investment, total system costs under V2G are 5.5% lower than without PEVs (a $360 per PEV per year reduction). When accounting for induced wind and solar capacity investment, total system costs under V2G are 16% lower than without PEVs (a $1000 per PEV per year reduction). The cost reduction per PEV per year is 14% higher than in the base case (a $880 per PEV per year reduction).

Though results indicate the magnitude of emission externality reduction benefits is quite sensitive to wind and solar generation profiles, the benefits persist to be significant (shown in Figure B.12). With higher solar capacity and lower wind capacity, total air emission externalities are reduced by $2300, 4.5% higher compared with the base case.

B.2.4.2 High wind scenario

Shown in Figure B.13, with more wind and less solar, the total wind and solar capacity investment induced by V2G changes notably, but capacity investment induction benefits persist and are even higher than the base case. Under a high wind scenario, V2G increases the maximum profitable capacity of wind and solar capacity by 17 GW (a 24% increase) for a combined wind and solar capacity of 71 GW with no PEVs. The increases are 13% higher than under the base case: 15 GW (a 23% increase) increase for a combined capacity with no PEVs of 64 GW.

As a result of higher induced wind and solar capacity investment, the wind and solar generation changes induced by V2G under the high battery scenario are also higher than in the base case (shown in Figure B.14). When induced capacity investment is

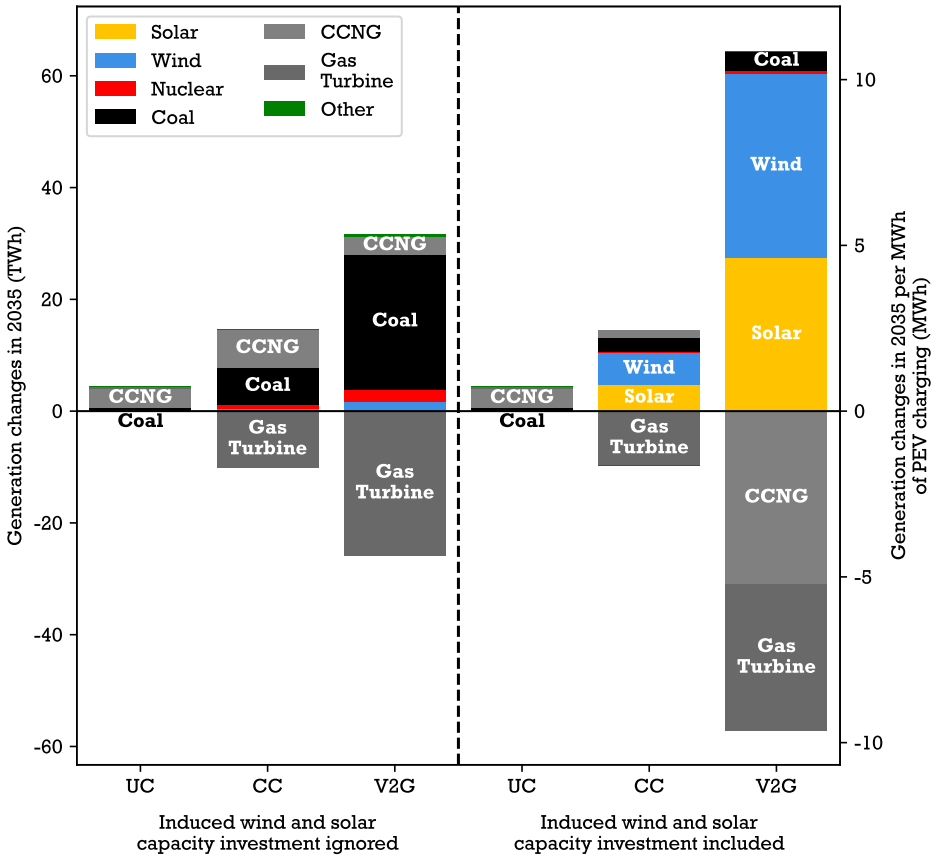


Figure B.11: Effect of PEV charging load on power generation. Changes in annual generation by fuel type, relative to the NoPEV case, for each PEV charging scenario when ignoring versus including induced wind and solar capacity investment. **All results in this figure are run with additional solar capacity and lower wind capacity.** All other parameters are the same. When accounting for induced wind and solar investment, wind and solar capacity and therefore generation vary across PEV charging scenarios. 'CCNG' fuel type includes combined cycle natural gas generators. 'Other' fuel types include biomass, fossil waste, fuel cell, hydro, landfill gas, municipal solid waste, non-fossil waste, and oil or gas steam.

considered, wind and solar generation increases (48 TWh) are 6.7% higher than under the base case (45 TWh).

When ignoring induced wind and solar capacity investment, total system costs under V2G are 5.5% lower than without PEVs (a $360 per PEV per year reduction). When accounting for induced wind and solar capacity investment, total system costs under V2G are 16% lower than without PEVs (a $1000 per PEV per year reduction). The cost reduction per PEV per year which is 14% higher than in the base case (a $880 per PEV

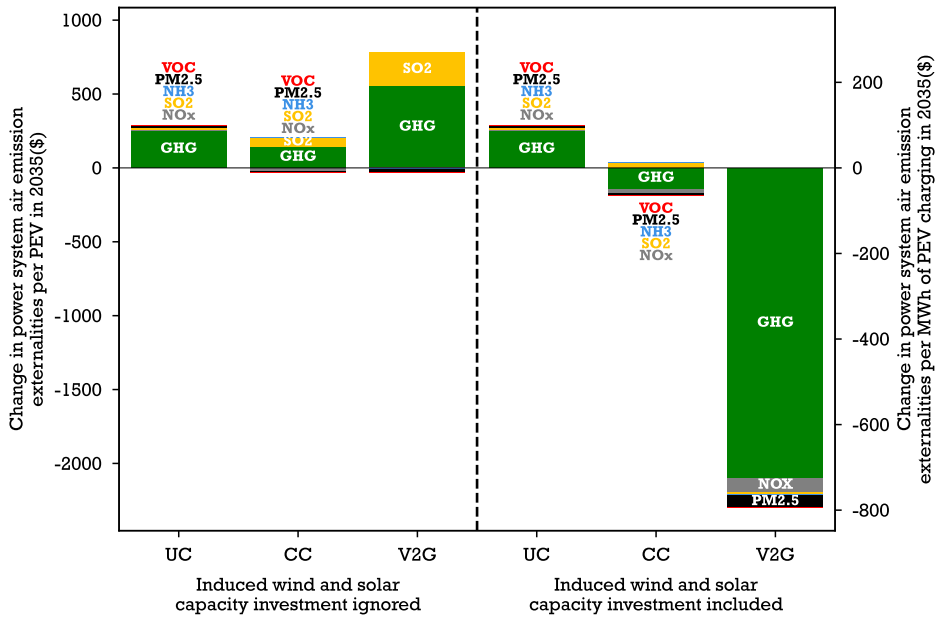


Figure B.12: Effect of PEV charging on power system air emission externalities. Change in total power system air emission externalities per PEV and per MWh of PEV charging in 2035, relative to the NoPEV scenario, under each PEV charging scenario when ignoring versus including induced wind and solar capacity investment. The 'ignored' scenarios use generation portfolios given by PJM's grid planning study for 2035 [24]. The 'included' scenarios consider wind and solar capacity at maximum profitable capacity, as described in Method and Materials. **All results in this figure are run with additional solar capacity and lower wind capacity.**

per year reduction).

Shown in Figure B.15. With higher solar capacity and lower wind capacity, total air emission externalities are reduced by $2300, 4% higher compared with the base case.

The two sets of sensitivity analysis results show that the magnitude of wind and solar capacity investment can be sensitive to wind and solar capacity buildout. As a result of different induced wind and solar capacity investments, system cost reduction benefits and emission reduction benefits can both be sensitive. However, in both sensitivity cases, all V2G benefits, including induced wind and solar capacity investment, system cost reduction benefits and emission reduction benefits, all persist and are higher than in the base case.

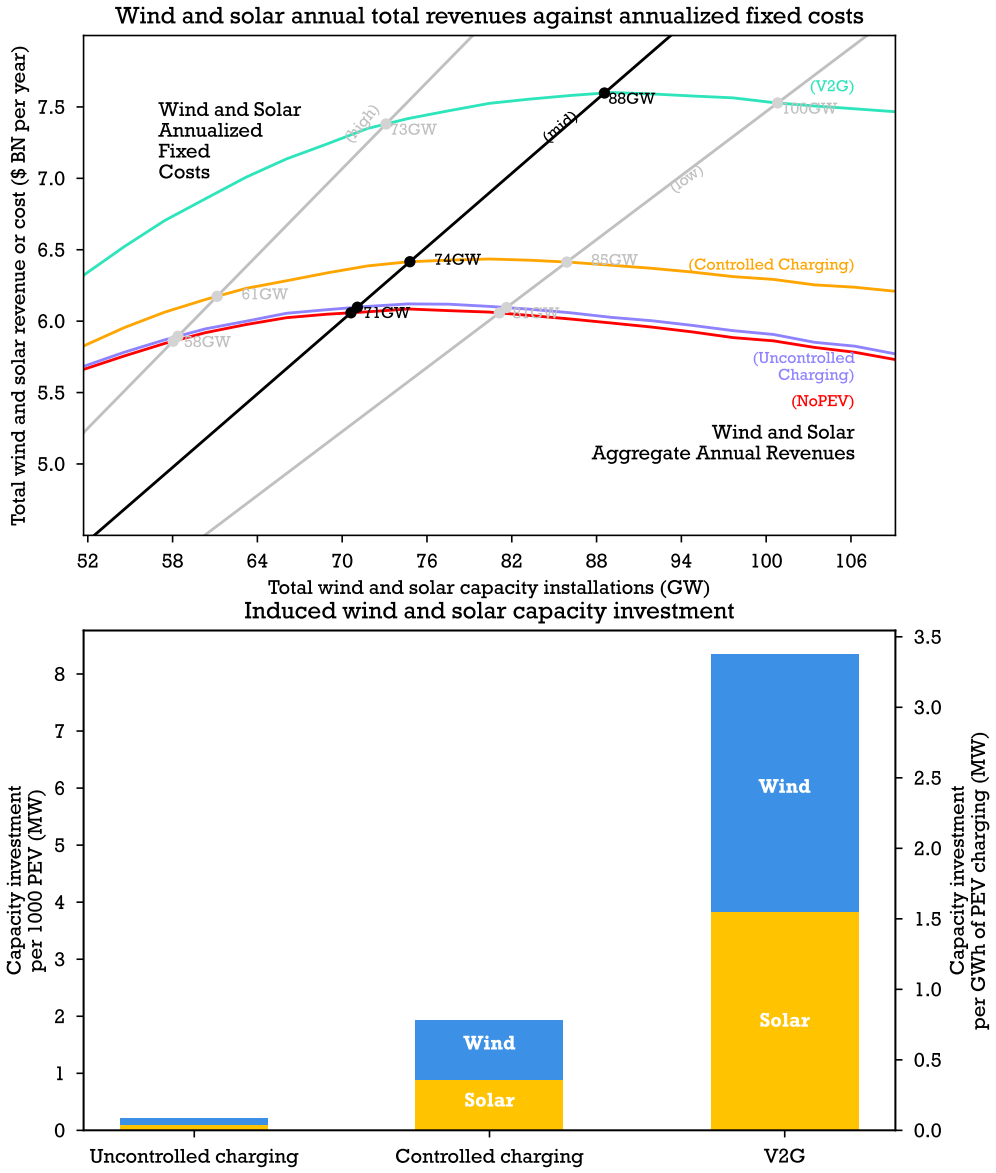


Figure B.13: Effect of PEV charging load on the economics of wind and solar capacity investment. Top panel: Total revenues and total annualized fixed costs for solar and wind generators, by PEV and PEV charging intervention scenarios and by wind and solar fixed cost scenarios. **All results in this figure are run with additional wind capacity and lower solar capacity.** All other parameters are the same. Note: (high): conservative fixed cost scenario, (mid): base case fixed cost scenario, (low): optimistic fixed cost scenario. Bottom panel: Wind and solar capacity investment induced by PEV charging interventions, including uncontrolled charging (UC), cost-minimizing charging (CC) and vehicle-to-grid (V2G), relative to the NoPEV baseline scenario. The currency unit is 2024 USD. $ BN is short for billion USD. Further detailed methods are described in the method section.

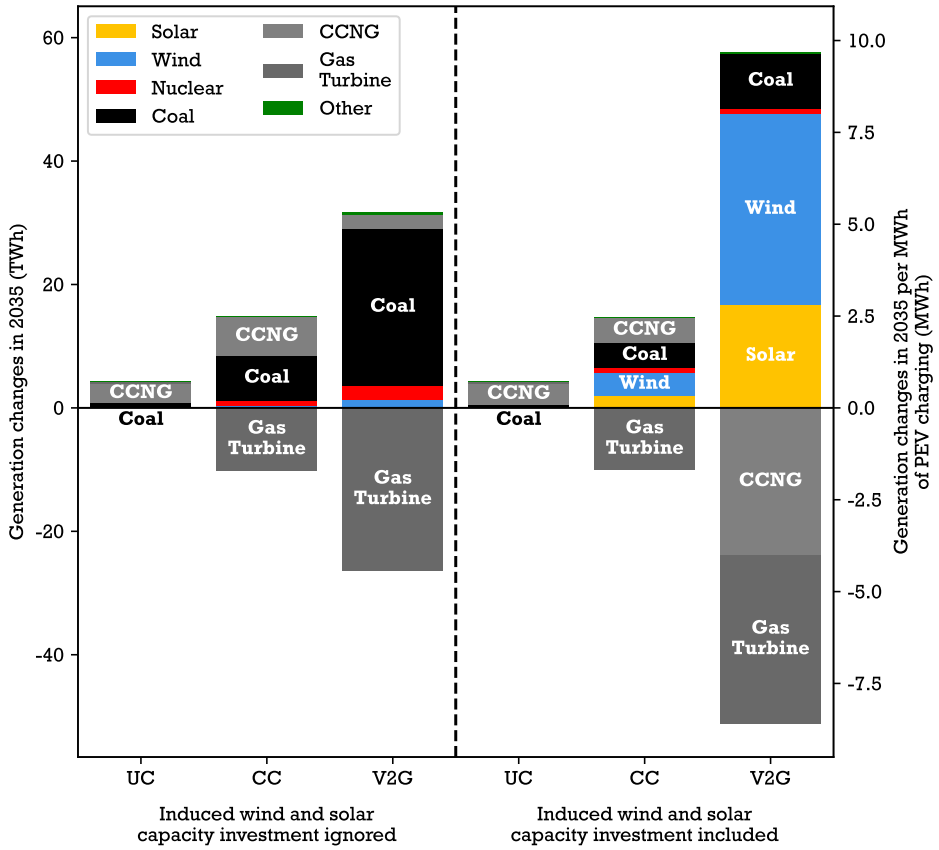


Figure B.14: Effect of PEV charging load on power generation. Changes in annual generation by fuel type, relative to the NoPEV case, for each PEV charging scenario when ignoring versus including induced wind and solar capacity investment. **All results in this figure are run with additional wind capacity and lower solar capacity.** All other parameters are the same. When accounting for induced wind and solar investment, wind and solar capacity and therefore generation vary across PEV charging scenarios. 'CCNG' fuel type includes combined cycle natural gas generators. 'Other' fuel types include biomass, fossil waste, fuel cell, hydro, landfill gas, municipal solid waste, non-fossil waste, and oil or gas steam.

B.3 Methods

B.3.1 Variable renewable energy cost estimation

We use cost modeling results from National Renewable Energy Laboratory's Annual Technology Baseline (ATB) database to assess fixed costs of solar and wind generators [25]. 2035 Conservative, Moderate, and Advanced scenarios in ATB correspond to Con-

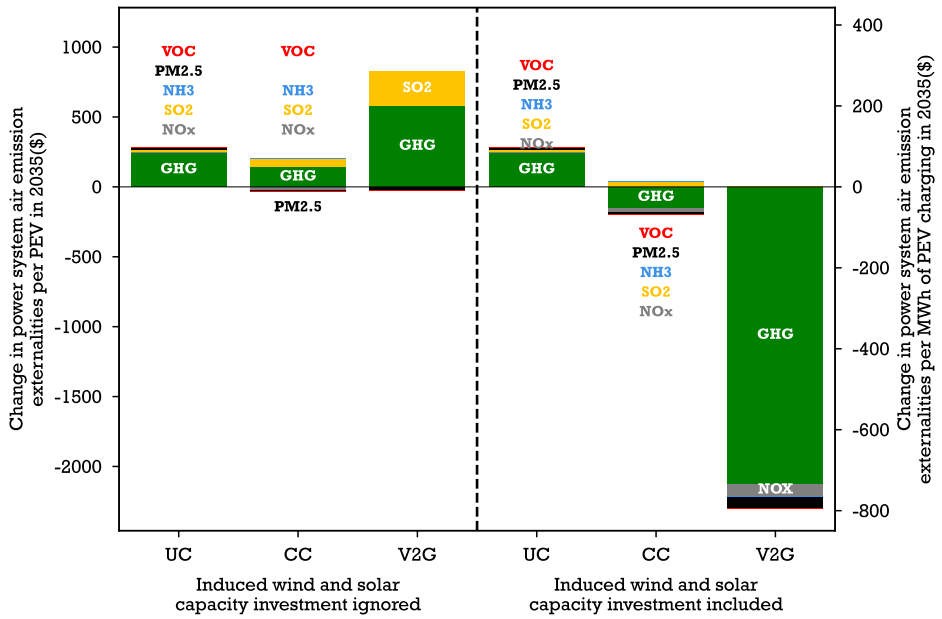


Figure B.15: Effect of PEV charging on power system air emission externalities. Change in total power system air emission externalities per PEV and per MWh of PEV charging in 2035, relative to the NoPEV scenario, under each PEV charging scenario when ignoring versus including induced wind and solar capacity investment. The 'ignored' scenarios use generation portfolios given by PJM's grid planning study for 2035 [24]. The 'included' scenarios consider wind and solar capacity at maximum profitable capacity, as described in Method and Materials. **All results in this figure are run with additional solar capacity and lower wind capacity.**

servative, Base case, and Optimistic scenarios in our study. Annualized capital costs are calculated with an interest rate of 5% and a capital recovery term of 30 years. The main results reported in the manuscript are based on the Base case scenario. Induced wind and solar capacity is also reported for Conservative and Advanced scenarios. The costs of three scenarios are shown in Table B.2.

B.3.2 PJM System Topography

The original modeling of the PJM Interconnection as 5 transmission constrained regions (TCR) was developed in Lueken et al. 2014 and Weis et al. 2014 [12], [26], which was later updated by Bruchon et al. 2024 [27]. The TCRs and transmission interfaces connecting TCRs are shown in Figure B.16. Transmission lines are aggregated into 5

Table B.2. Capital expenditures and fixed O&M costs of wind and power sources in 2024 USD, under different cost scenarios [25]

Technology		Optimistic	Base case	Conservative
On-shore wind	Capital expenditures (USD/kW)	1034	1093	1231
	Annual O&M (USD/kW)	21.6	26.1	28.1
Off-shore wind	Capital expenditures (USD/kW)	2397	2709	3414
	Annual O&M (USD/kW)	75.1	84.5	104.8
Solar	Capital expenditures (USD/kW)	632	829	1101
	Annual O&M (USD/kW)	13.1	15.5	18.9

inter-regional transmission interfaces, shown in Figure B.17. Transmission capacity of each interfaces are extracted from PJM website (PJM Data Miner).

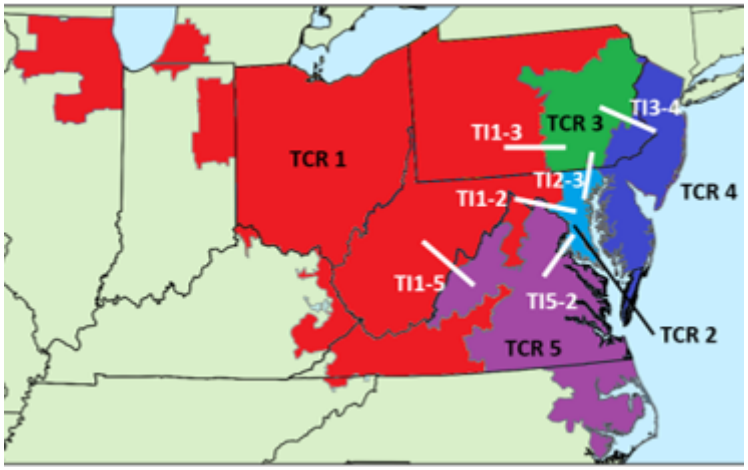


Figure B.16: Map of Transmission Constrained Regions (TCRs) and Transmission Interconnections (TIs).

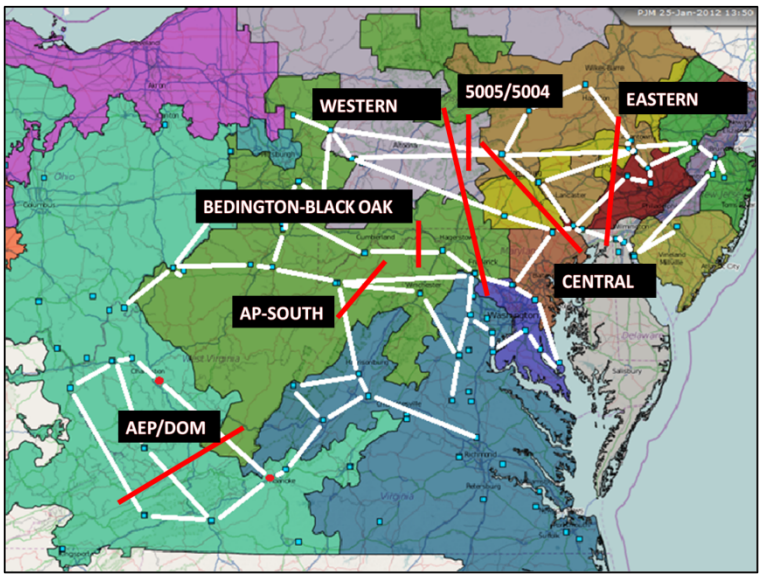


Figure B.17: Map of PJM 500kV transmission lines (white lines) and transmission interfaces (red lines). Most interfaces contain multiple 500kV lines. The map illustrates model representation of PJM in Bruchon et al. 2024.

B.3.3 Power system model formulation

Table B.3. Nomenclature: sets, decision variables, and input parameters. The nomenclature is for optimization problem formulations. The problem formulation describes the unit commitment economic dispatch model that simulates hourly simulation of PJM' s power system for one year.

Label	Type	Description
$\mathcal{I}$	Set	Generating units
$\mathcal{K}$	Set	Storage units
$\mathcal{R}$	Set	Transmission constraint regions (TCRs)
$\mathcal{T}$	Set	Timesteps
$\mathcal{V}$	Set	Plug-in electric vehicle schedule groups
$c^{\text{VEH}}_{v,r,t}$	Variable	Charge level (MWh) of vehicle schedule group v in TCR r at time t
$c^{\text{STR}}_{k,t}$	Variable	Charge level (MWh) of storage unit k at time t
$p^{\text{GEN}}_{i,t}$	Variable	Power generated by unit i at time t
$p^{\text{SGEN}}_{r,t}$	Variable	Power generated by solar PV generators in TCR r at time t
$p^{\text{WGEN}}_{r,t}$	Variable	Power generated by wind generators in TCR r at time t
$p^{\text{STRD}}_{k,t}$	Variable	Power discharged (+) by storage unit k at time t
$p^{\text{STRC}}_{k,t}$	Variable	Power charged (+) by storage unit k at time t
$p^{\text{RR}}_{r,r',t}$	Variable	Power imported (+) from TCR r' to TCR $r(r \neq r')$ at time t
$p^{\text{VR}}_{v,r,t}$	Variable	Power charged (+) by vehicle schedule group v in TCR r at time t
$p^{\text{DR}}_{v,r,t}$	Variable	Power discharged (+) by vehicle schedule group v in TCR r at time t
$a^{\text{GEN}}_{i,t}$	Variable	Reserve provided by generator unit i at time t
$a^{\text{STR}}_{k,t}$	Variable	Reserve provided by storage unit k at time t
$a^{\text{VR}}_{v,r,t}$	Variable	Reserve provided by vehicle schedule group v in TCR r at time t
$a^{\text{GENSP}}_{i,t}$	Variable	Spinning reserve provided by generator unit i at time t
$a^{\text{STRSP}}_{k,t}$	Variable	Spinning reserve provided by storage unit k at time t
$a^{\text{VRSP}}_{v,r,t}$	Variable	Spinning reserve provided by vehicle schedule group v in TCR r at time t
$s^{\text{STARTUP}}_{i,t}$	Variable	Slack variable for startup cost
$u_{i,t}$	Variable	Binary variable that is equal to 1 if unit i is online in period t and 0 otherwise
$A_{v,t}$	Parameter	Availability of vehicle schedule group v to charge at time t (%)
B_v	Parameter	Battery capacity (MWh) of vehicle grouping v
c^{STRMAX}_{k}	Parameter	Max charge level (MWh) of storage unit k
c^{STRMIN}_{k}	Parameter	Min charge level (MWh) of storage unit k
C^{STR}	Parameter	Reserve provision cost of storage unit
C^{VEH}	Parameter	Reserve provision cost of PEV
C^{VARGEN}_{i}	Parameter	Variable cost of generating unit i
C^{STARTGEN}_{i}	Parameter	Startup cost of generating unit i
$p^{\text{SGENMAX}}_{r,t}$	Parameter	Maximum power generated by solar PV generators in TCR r at time t
$p^{\text{WGENMAX}}_{r,t}$	Parameter	Maximum power generated by wind generators in TCR r at time t
$P_{r,t}$	Parameter	Power demand in TCR r at time t
$p^{\text{RRMAX}}_{r,r',t}$	Parameter	Max power flow on interface (r, r') at time t
$M_{v,t}$	Parameter	Miles traveled per car in vehicle schedule group v at time t
$N_{v,r}$	Parameter	Number of vehicles in schedule group v in TCR r
p^{GENMIN}_{i}	Parameter	Min generation from unit i at time t
p^{GENMAX}_{i}	Parameter	Max generation from unit i at time t
p^{STRMAX}_{k}	Parameter	Max discharge rate from storage unit k
R_i	Parameter	Ramp rate limit of unit i
R^{MAXCHG}_{v}	Parameter	Max charge rate (MW) of vehicle schedule group v
T^{UPMIN}_{i}	Parameter	Minimum uptime of unit i
T^{DTMIN}_{i}	Parameter	Minimum downtime of unit i
C^{GENRES}_{i}	Parameter	Reserve provision cost of unit i
T^{UPSTART}_{i}	Parameter	Number of timesteps unit i has been online at initial timestep $t = 1$
T^{DTSTART}_{i}	Parameter	Number of timesteps unit i has been offline at initial timestep $t = 1$
T^{DEPART}_{v}	Parameter	Timestep at which vehicle schedule group v departs home
η^{CHG}_{v}	Parameter	Charging and discharging efficiency (%) of vehicle schedule group v
η^{STR}_{k}	Parameter	Efficiency (%) of storage unit k
η^{VEH}_{v}	Parameter	Driving efficiency (MWh/mile) of vehicle schedule group v
η^{TR}	Parameter	Transmission efficiency (%)
p^{S}_{r}	Parameter	Solar PV capacity of region r (MW)
ϕ^{REG}	Parameter	Ratio of load regulation reserve requirement to load (%)
ϕ^{WIND}	Parameter	Ratio of wind regulation reserve requirement to regional wind generation (%)
ϕ^{SOL}	Parameter	Ratio of solar PV regulation reserve requirement to regional solar PV installed capacity (%)
ϕ^{SPIN}	Parameter	Ratio of spinning reserve requirement to load (%)

We in this study updated and adapted the unit commitment economic dispatch model formulation of Weis. et al. 2016 and Bruchon et al. 2024 to enable V2G functionalities [27], [28]. The mixed integer optimization problem is formulated as follows:

Optimization problem formulation. The problem formulation describes the unit commitment economic dispatch model that simulates hourly simulation of PJM' s power system for one year.

$$\begin{aligned}\text{Minimize } Z = &\sum_{t\in\mathcal{T}}\sum_{i\in I_r}\left(C_i^{\text{VARGEN}}p_{i,t}^{\text{GEN}} + s_{i,t}^{\text{STARTUP}} + C_i^{\text{GENRES}}a_{i,t}^{\text{GEN}}\right)\\ &+\sum_{t\in\mathcal{T}}\sum_{k\in\mathcal{K}}C^{\text{STR}}a_{k,t}^{\text{STR}} + \sum_{t\in\mathcal{T}}\sum_{v\in\mathcal{V}}\sum_{r\in\mathcal{R}}C^{\text{VEH}}a_{v,r,t}^{\text{VEH}}\end{aligned} \tag{B.1}$$

Subject to

Generator constraints:

$$a_{i,t}^{\text{GEN}} \le 1/12 * \left(p_{i,t-1} + R_i u_{i,t} + p_i^{\text{GENMIN}}(u_{i,t} - u_{i,t-1}) - p_{i,t}\right) - a_{i,t}^{\text{GENSP}}$$
$$\forall i \in \mathcal{I} \neq 1, \forall t \in \mathcal{T} \quad \text{Generator regulation reserve offer constraints} \tag{B.2}$$

$$a_{i,t}^{\text{GEN}} \le 1/12 * \left(p_i^{\text{GENMAX}} - p_{i,t}\right) - a_{i,t}^{\text{GENSP}}$$
$$\forall i \in \mathcal{I} \neq 1, \forall t \in \mathcal{T} \quad \text{Generator regulation reserve offer constraints} \tag{B.3}$$

$$a_{i,t}^{\text{GEN}} \le 1/12 * \left(p_i^{\text{GENMAX}} u_{i,t}\right) - a_{i,t}^{\text{GENSP}}$$
$$\forall i \in \mathcal{I} \neq 1, \forall t \in \mathcal{T} \quad \text{Generator regulation reserve offer constraints} \tag{B.4}$$

$$a_{i,t}^{\text{GENSP}} \le 1/6 * \left(p_{i,t-1} + R_i u_{i,t} + p_i^{\text{GENMIN}}(u_{i,t} - u_{i,t-1}) - p_{i,t}\right) - a_{i,t}^{\text{GENSP}}$$
$$\forall i \in \mathcal{I} \neq 1, \forall t \in \mathcal{T} \quad \text{Generator spinning reserve offer constraints} \tag{B.5}$$

$$a_{i,t}^{\text{GENSP}} \le 1/6 * \left(p_i^{\text{GENMAX}} - p_{i,t}\right) - a_{i,t}^{\text{GEN}}$$
$$\forall i \in \mathcal{I} \neq 1, \forall t \in \mathcal{T} \quad \text{Generator spinning reserve offer constraints} \tag{B.6}$$

$$a_{i,t}^{\text{GENSP}} \le 1/6 * \left(p_i^{\text{GENMAX}} u_{i,t}\right) - a_{i,t}^{\text{GEN}}$$
$$\forall i \in \mathcal{I} \neq 1, \forall t \in \mathcal{T} \quad \text{Generator spinning reserve offer constraints} \tag{B.7}$$

$$s_{i,t}^{\text{STARTUP}} \ge \left(u_{i,t} - u_{i,t-1}\right) C_i^{\text{STARTGEN}}$$

$\forall i \in \mathcal{I}, \forall t \in \mathcal{T}$ Slack variable reflects startup decision (B.8)

$$s_{i,t}^{\text{STARTUP}} \geq 0$$

$\forall i \in \mathcal{I}, \forall t \in \mathcal{T}$ Slack variable is nonnegative (B.9)

$$p_i^{\text{GENMIN}} u_{i,t} \leq p_{i,t} \leq p_i^{\text{GENMAX}} u_{i,t}$$

$\forall i \in \mathcal{I}, \forall t \in \mathcal{T}$ Min and max output of online generators (B.10)

$$p_{i,t}^{\text{GEN}} \leq p_{i,t-1}^{\text{GEN}} + R_i u_{i,t-1} + p_i^{\text{GENMIN}} \left(u_{i,t} - u_{i,t-1}\right)$$

$\forall i \in \mathcal{I}, \forall t \in \mathcal{T}$ Ramp rate limit (B.11)

$$p_{i,t-1}^{\text{GEN}} \leq p_{i,t}^{\text{GEN}} + R_i u_{i,t} + p_i^{\text{GENMIN}} \left(u_{i,t-1} - u_{i,t}\right)$$

$\forall i \in \mathcal{I}, \forall t \in \mathcal{T}$ Ramp rate limit (B.12)

$$\sum_{t=2}^{T_i^{\text{UPMIN}} - T_i^{\text{UPSTART}}} (1 - u_{i,t}) = 0$$

$\forall i \in \mathcal{I}$ Minimum uptime (first timesteps) (B.13)

$$\sum_{t'=t}^{t+T_i^{\text{UPMIN}}-1} u_{i,t'} \geq T_i^{\text{UPMIN}} \left(u_{i,t} - u_{i,t-1}\right)$$

$\forall i \in \mathcal{I},$

$\forall t : T_i^{\text{UPMIN}} - T_i^{\text{UPSTART}} + 1 \leq t \leq |\mathcal{T}| - T_i^{\text{UPMIN}} + 1$

Minimum uptime (middle timesteps) (B.14)

$$\sum_{t=t}^{T} u_{i,t'} \geq (T - t) \left(u_{i,t} - u_{i,t-1}\right)$$

$\forall i \in \mathcal{I},$

$\forall t \in |\mathcal{T}| - T_i^{\text{UPMIN}} + 2 \ldots$ Minimum uptime (final timesteps) (B.15)

$$\sum_{t=2}^{T_i^{\text{DTMIN}} - T_i^{\text{DTSTART}}} u_{i,t} = 0$$

$\forall i \in \mathcal{I}$ Minimum downtime (first timesteps) (B.16)

$$\sum_{t'=t}^{t+T_i^{\text{DTMIN}}-1} 1 - u_{i,t'} \geq T_i^{\text{DTMIN}} \left(u_{i,t-1} - u_{i,t}\right)$$

$\forall i \in \mathcal{I},$

$\forall t : T_i^{\text{DTSTART}} + 1 \leq t \leq |\mathcal{T}| - T_i^{\text{DTSTART}} + 1$

Minimum downtime (middle timesteps) (B.17)

$$\sum_{t'=t}^{T} 1 - u_{i,t'} \geq (|\mathcal{T}| - t)\,(u_{i,t-1} - u_{i,t})$$
$$\forall i \in \mathcal{I},$$
$$\forall t : |\mathcal{T}| - T_i^{\text{DTSTART}} + 2 \leq t \leq |\mathcal{T}|$$
Minimum downtime (final timesteps) (B.18)

$$\text{Minimize } Z = \sum_{t\in\mathcal{T}} \sum_{i\in I_r} \left(C_i^{\text{VARGEN}} p_{i,t}^{\text{GEN}} + s_{i,t}^{\text{STARTUP}} + C_i^{\text{GENRES}} a_{i,t}^{\text{GEN}}\right) + \sum_{t\in\mathcal{T}} \sum_{k\in\mathcal{K}} C_k^{\text{STR}} a_{k,t}^{\text{STR}} + \sum_{t\in\mathcal{T}} \sum_{v\in\mathcal{V}} \sum_{r\in\mathcal{R}} C^{\text{VEH}} a_{v,r,t}^{\text{VEH}}$$

Subject to

System constraints:

$$P_{r,t} = \sum_{i\in\mathcal{I}_r} p_{i,t}^{\text{GEN}} + \sum_{k\in\mathcal{K}_r} p_{i,t}^{\text{STRD}} - \sum_{k\in\mathcal{K}_r} p_{i,t}^{\text{STRC}} - \sum_{r'\in\mathcal{R}\neq r} (p_{r',r,t}^{\text{RR}}) + \sum_{r'\in\mathcal{R}\neq r} (p_{r,r',t}^{\text{RR}} \eta^{\text{TR}}) + p_{r,t}^{\text{SGEN}} + p_{r,t}^{\text{WGEN}} - \sum_{v\in\mathcal{V}_r} p_{v,r,t}^{\text{VR}} + \sum_{v\in\mathcal{V}_r} p_{v,r,t}^{\text{DR}}$$
$$\forall r \in \mathcal{R}, t \in \mathcal{T} \quad \text{Demand must equal supply} \tag{B.19}$$

$$-p_{r,r',t}^{\text{RRMAX}} \leq p_{r,r',t}^{\text{RR}} \leq p_{r,r',t}^{\text{RRMAX}}$$
$$\forall r \in \mathcal{R}, r' \in \mathcal{R} \neq r, t \in \mathcal{T} \quad \text{Inter-region power flow limits} \tag{B.20}$$

$$0 \leq p_{r,t}^{\text{SGEN}} \leq p_{r,t}^{\text{SGENMAX}}$$
$$\forall r \in \mathcal{R}, t \in \mathcal{T} \quad \text{Regional solar PV output limits} \tag{B.21}$$

$$0 \leq p_{r,t}^{\text{WGEN}} \leq p_{r,t}^{\text{WGENMAX}}$$
$$\forall r \in \mathcal{R}, t \in \mathcal{T} \quad \text{Regional wind generator output limits} \tag{B.22}$$

$$\phi^{SPIN} * P_{r,t} = \sum_{i\in\mathcal{I}_r} a_{i,t}^{\text{GENSP}} + \sum_{k\in\mathcal{K}_r} a_{k,t}^{\text{STRSP}} + \sum_{v\in\mathcal{V}_r} a_{v,r,t}^{\text{VRSP}}$$
$$\forall r \in \mathcal{R}, t \in \mathcal{T} \quad \text{Regional spinning reserve requirement must be met} \tag{B.23}$$

$$\phi^{REG} * P_{r,t} + \phi^{\text{WIND}} * p_{r,t}^{\text{WGEN}} + \phi^{\text{SOL}} * p^{\text{S}} = \sum_{i \in \mathcal{I}_r} a_{i,t}^{\text{GEN}} + \sum_{k \in \mathcal{K}_r} a_{k,t}^{\text{STR}} + \sum_{v \in \mathcal{V}_r} a_{v,r,t}^{\text{VR}}$$

$$\forall r \in \mathcal{R}, t \in \mathcal{T} \quad \text{Regional regulation reserve requirement must be met} \tag{B.24}$$

Storage constraints:

$$c_{k,t+1}^{\text{STR}} = c_{k,t}^{\text{STR}} + p_{k,t}^{\text{STRC}} \eta^{STR} - p_{k,t}^{\text{STRD}} / \eta^{STR}$$

$$\forall k \in \mathcal{K}, \forall t \in \mathcal{T} \quad \text{Storage state of charge} \tag{B.25}$$

$$c_k^{\text{STRMIN}} \leq c_{k,t}^{\text{STR}} \leq c_k^{\text{STRMAX}}$$

$$\forall k \in \mathcal{K}, \forall t \in \mathcal{T} \quad \text{Storage unit capacity} \tag{B.26}$$

$$0 \leq p_{k,t}^{\text{STRD}}, p_{k,t}^{\text{STRC}} \leq p_k^{\text{STRMAX}}$$

$$\forall k \in \mathcal{K}, \forall t \in \mathcal{T} \quad \text{Max charge and discharge of storage units} \tag{B.27}$$

$$a_{k,t}^{\text{STRSP}} \leq p_k^{\text{STRMAX}} - p_{k,t}^{\text{STRD}} + p_{k,t}^{\text{STRC}} - a_{k,t}^{\text{STR}}$$

$$\forall k \in \mathcal{K}, \forall t \in \mathcal{T} \quad \text{Max regulation and spinning reserve offer of storage units} \tag{B.28}$$

$$a_{k,t}^{\text{STRSP}} \leq c_{k,t}^{\text{STR}} - a_{k,t}^{\text{STR}}$$

$$\forall k \in \mathcal{K}, \forall t \in \mathcal{T} \quad \text{Max regulation and spinning reserve offer of storage units} \tag{B.29}$$

PEV constraints:

$$c_{v,r,t+1}^{\text{VEH}} = c_{v,r,t}^{\text{CHG}} - p_{v,r,t}^{\text{VR}} \eta_v^{\text{VEH}} - N_{v,r} M_{v,t} \eta_v^{\text{VEH}}$$

$$\forall v \in \mathcal{V}, \forall r \in \mathcal{R}, \forall t \in \mathcal{T} \quad \text{PEV state of charge} \tag{B.30}$$

$$10\% N_{v,r} B_v \leq c_{v,r,t}^{\text{VEH}} \leq 90\% N_{v,r} B_v$$

$$\forall v \in \mathcal{V}, \forall r \in \mathcal{R}, \forall t \in \mathcal{T} \quad \text{PEV battery capacity} \tag{B.31}$$

$$c_{v,r,t}^{\text{VEH}} = 90\% N_{v,r} B_v$$

$$\forall v \in \mathcal{V}, \forall r \in \mathcal{R}, \forall t = T_v^{\text{DEPART}} \quad \text{PEVs fully charged when departing home} \tag{B.32}$$

$$c^{\mathrm{VEH}}_{v,r,t+1} = c^{\mathrm{CHG}}_{v,r,t} - p^{\mathrm{VR}}_{v,r,t}/\eta^{\mathrm{CHG}}_{v} + p^{\mathrm{DR}}_{v,r,t} * \eta^{\mathrm{CHG}}_{v} N_{v,r} M_{v,t} \eta^{\mathrm{VEH}}_{v}$$

$$\forall v \in \mathcal{V}, \forall r \in \mathcal{R}, \forall t \in \mathcal{T} \quad \text{PEV state of charge} \tag{B.33}$$

$$0 \leq p^{\mathrm{VR}}_{v,r,t}, p^{\mathrm{DR}}_{v,r,t} \leq N_{v,r} A_{v,t} R^{\mathrm{MAXCHG}}_{v}$$

$$\forall v \in \mathcal{V}, \forall r \in \mathcal{R}, \forall t \in \mathcal{T} \quad \text{PEV charge rate limit} \tag{B.34}$$

$$0 \leq c^{\mathrm{VEH}}_{v,r,t} \leq N_{v,r} B_{v}$$

$$\forall v \in \mathcal{V}, \forall r \in \mathcal{R}, \forall t \in \mathcal{T} \quad \text{PEV battery capacity} \tag{B.35}$$

$$a^{\mathrm{VRSP}}_{v,r,t} \leq N_{v,r} A_{v,t} R^{\mathrm{MAXCHG}}_{v} - p^{\mathrm{DR}}_{v,r,t} + p^{\mathrm{VR}}_{v,r,t} - a^{\mathrm{VR}}_{v,r,t}$$

$$\forall r \in \mathcal{R}, \forall v \in \mathcal{V} \quad \text{Max regulation and spinning reserve offer of vehicle fleets} \tag{B.36}$$

$$a^{\mathrm{VRSP}}_{v,r,t} \leq c^{\mathrm{VEH}}_{v,r,t} - a^{\mathrm{VR}}_{v,r,t}$$

$$\forall r \in \mathcal{R}, \forall v \in \mathcal{V}, \forall t \in \mathcal{T} \tag{B.37}$$

This study models two reserve products: regulation reserve (5min) and spinning reserve (10min). For the calculation of these requirements, we adopt the parameters developed by the National Renewable Energy Laboratory (NREL) ReEDS model [29]. The reserve provision costs account for variable costs incurred by degraded heat rate and other factors, and we adopt the parameters used by NREL's ReEDS model and Craig et al. 2017 (seen in Table B.4) [29], [30].

Table B.4. Reserve provisional costs of different reserve providers by fuel type or technology type

Fuel and technology type	Coal	Combined Cycle Natural Gas	Gas/Oil steam	Storage	Storage by PEV
Cost($/MWh)	10	6	4	2	2

B.4 More results

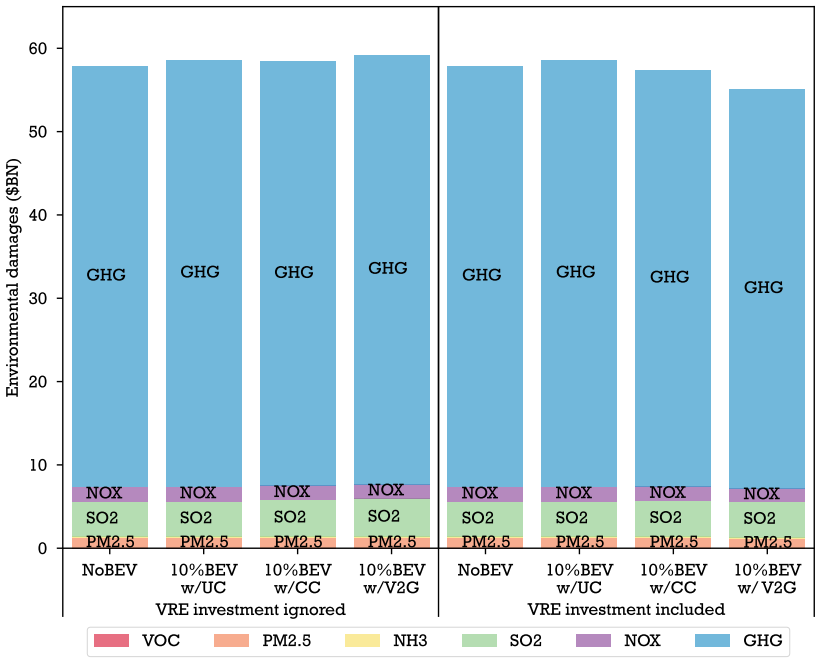


Figure B.18: Annual environmental externalities of GHG emissions and pollution, by different PEV and PEV charging intervention scenarios and analysis approaches. Wind and power capacity varies across PEV and PEV charging intervention scenarios in Expansion scenarios, as PEV and PEV charging intervention affects the maximum profitable wind and power capacity installation. Environmental externalities for GHG emissions are calculated with social cost of carbon of \$204/ton CO_2e in 2023, published by US Environment Protection Agency[31]. The results with a lower cost of carbon of \$51/ton CO_2e can be found in SI. The AP3 model is used to calculate those of pollutants.

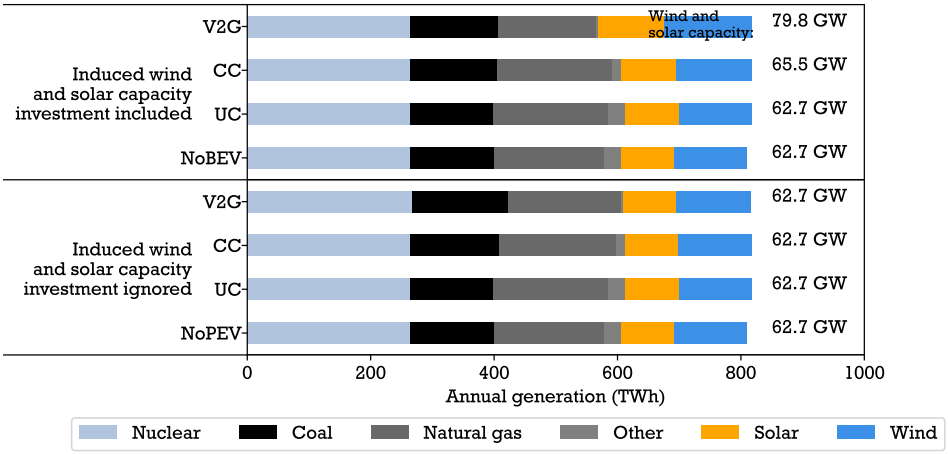


Figure B.19: Annual generation of different fuel types, by different PEV and PEV charging intervention scenarios and analysis approaches. Wind and solar capacity varies across PEV and PEV charging intervention scenarios in wind and solar capacity investment scenarios, as PEV and PEV charging interventions affect the maximum profitable wind and solar capacity installations. 'Natural gas' fuel type includes combined cycle natural gas generators and gas turbine generators. 'Other' fuel types include biomass, fossil waste, fuel cell, hydro, landfill gas, municipal solid waste, non-fossil waste, and oil or gas steam.

Table B.5. Annual emissions and environmental externalities of greenhouse gases and air pollutants, by different grid intervention scenarios and analysis approaches. wind and power capacity varies across grid intervention scenarios in wind and power scenarios, as PEV charging intervention intervention affects the maximum profitable wind and power capacity installation. Environmental externalities for GHG emissions are calculated with social cost of carbon of \$204/ton CO_2e. The AP3 model is used to calculate those of pollutants. All costs are in 2024 USD.

			Emission Externalities (\$MM)					
			GHG	NOx	SO2	NH3	PM25	VOC
Wind and Solar Capacity Investment	Ignored	NoPEV	50455	1765	4195	165	1208	14
		Uncontrolled charging	51152	1771	4206	182	1246	15
		Cost-minimizing charging	50895	1685	4380	181	1199	13
		V2G	51467	1730	4595	180	1182	13
	Included	NoPEV	50455	1765	4195	165	1208	14
		Uncontrolled charging	51152	1771	4206	182	1246	15
		Cost-minimizing charging	50013	1662	4286	178	1180	13
		V2G	46155	1568	4128	163	1052	12

References

[1] S. P. Holland, M. J. Kotchen, E. T. Mansur, and A. J. Yates, "Why marginal CO2 emissions are not decreasing for US electricity: Estimates and implications for climate policy," *Proceedings of the National Academy of Sciences*, vol. 119, no. 8, e2116632119, Feb. 2022, Publisher: Proceedings of the National Academy of Sciences. DOI: 10.1073/pnas.2116632119. Accessed: Feb. 3, 2024. [Online]. Available: https://www.pnas.org/doi/abs/10.1073/pnas.2116632119 .

[2] R. Tu, Y. (Gai, B. Farooq, D. Posen, and M. Hatzopoulou, "Electric vehicle charging optimization to minimize marginal greenhouse gas emissions from power generation," en, *Applied Energy*, vol. 277, p. 115 517, Nov. 2020, ISSN: 0306-2619. DOI: 10.1016/j.apenergy.2020.115517. Accessed: Oct. 4, 2020. [Online]. Available: http://www.sciencedirect.com/science/article/pii/S0306261920310291 .

[3] J. Chen, F. Wang, X. He, X. Liang, J. Huang, S. Zhang, and Y. Wu, "Emission mitigation potential from coordinated charging schemes for future private electric vehicles," en, *Applied Energy*, vol. 308, p. 118 385, Feb. 2022, ISSN: 0306-2619. DOI: 10.1016/j.apenergy.2021.118385. Accessed: Mar. 22, 2022. [Online]. Available: https://www.sciencedirect.com/science/article/pii/S0306261921016238 .

[4] M. Wang and M. T. Craig, "The value of vehicle-to-grid in a decarbonizing California grid," en, *Journal of Power Sources*, vol. 513, p. 230 472, Nov. 2021, ISSN: 0378-7753. DOI: 10.1016/j.jpowsour.2021.230472. Accessed: Jul. 1, 2023. [Online]. Available: https://www.sciencedirect.com/science/article/pii/S0378775321009757 .

[5] R. Shi, S. Li, P. Zhang, and K. Y. Lee, "Integration of renewable energy sources and electric vehicles in V2G network with adjustable robust optimization," *Renewable Energy*, vol. 153, pp. 1067–1080, Jun. 2020, ISSN: 0960-1481. DOI: 10.1016/j.renene.2020.02.027. Accessed: Apr. 25, 2024. [Online]. Available: https://www.sciencedirect.com/science/article/pii/S0960148120302135 .

[6] N. A. Ryan, J. X. Johnson, and G. A. Keoleian, "Comparative Assessment of Models and Methods To Calculate Grid Electricity Emissions," *Environmental Science & Technology*, vol. 50, no. 17, pp. 8937–8953, Sep. 2016, Publisher: American Chemical Society, ISSN: 0013-936X. DOI: 10.1021/acs.est.5b05216. Accessed: Mar. 5, 2024. [Online]. Available: https://doi.org/10.1021/acs.est.5b05216 .

[7] X. Chen, H. Zhang, Z. Xu, C. P. Nielsen, M. B. McElroy, and J. Lv, "Impacts of fleet types and charging modes for electric vehicles on emissions under different penetrations of wind power," *Nature Energy*, vol. 3, no. 5, pp. 413–421, 2018, Publisher: Nature Publishing Group.

[8] J. Owens, I. Miller, and E. Gençer, "Can vehicle-to-grid facilitate the transition to low carbon energy systems?" en, *Energy Advances*, vol. 1, no. 12, pp. 984–998, 2022. DOI: 10.1039/D2YA00204C. Accessed: Jun. 20, 2023. [Online]. Available: https://pubs.rsc.org/en/content/articlelanding/2022/ya/d2ya00204c .

[9] P. Gagnon and W. Cole, "Planning for the evolution of the electric grid with a long-run marginal emission rate," *iScience*, vol. 25, no. 3, p. 103 915, Mar. 2022, ISSN: 2589-0042. DOI: 10.1016/j.isci.2022.103915. Accessed: Feb. 12, 2024. [Online]. Available: https://www.sciencedirect.com/science/article/pii/S2589004222001857 .

[10] T. Brown, D. Schlachtberger, A. Kies, S. Schramm, and M. Greiner, "Synergies of sector coupling and transmission reinforcement in a cost-optimised, highly renewable European energy system," *Energy*, vol. 160, pp. 720–739, Oct. 2018, ISSN: 0360-5442. DOI: 10.1016/j.energy.2018.06.222. Accessed: Feb. 12, 2024. [Online]. Available: https://www.sciencedirect.com/science/article/pii/S036054421831288X .

[11] F. Manríquez, E. Sauma, J. Aguado, S. de la Torre, and J. Contreras, "The impact of electric vehicle charging schemes in power system expansion planning," *Applied Energy*, vol. 262, p. 114 527, Mar. 2020, ISSN: 0306-2619. DOI: 10.1016/j.apenergy.2020.114527. Accessed: Feb. 12, 2024. [Online]. Available: https://www.sciencedirect.com/science/article/pii/S0306261920300398 .

[12] A. Weis, P. Jaramillo, and J. Michalek, "Estimating the potential of controlled plug-in hybrid electric vehicle charging to reduce operational and capacity expansion costs for electric power systems with high wind penetration," en, *Applied Energy*, vol. 115, pp. 190–204, Feb. 2014, ISSN: 0306-2619. DOI: 10.1016/j.apenergy.2013.10.017. Accessed: Nov. 27, 2021. [Online]. Available: https://www.sciencedirect.com/science/article/pii/S0306261913008374 .

[13] E. S. Hittinger and I. M. L. Azevedo, "Bulk Energy Storage Increases United States Electricity System Emissions," *Environmental Science & Technology*, vol. 49, no. 5, pp. 3203–3210, Mar. 2015, ISSN: 0013-936X. DOI: 10.1021/es505027p. Accessed: Apr. 27, 2024. [Online]. Available: https://doi.org/10.1021/es505027p .

[14] M. Muratori, "Impact of uncoordinated plug-in electric vehicle charging on residential power demand," *Nature Energy*, vol. 3, no. 3, pp. 193–201, 2018, Publisher: Nature Publishing Group.

[15] M. E. Kahn and R. K. Vaughn, "Green Market Geography: The Spatial Clustering of Hybrid Vehicles and LEED Registered Buildings," en, *The B.E. Journal of Economic Analysis & Policy*, vol. 9, no. 2, Mar. 2009, Publisher: De Gruyter, ISSN: 1935-1682. DOI: 10.2202/1935-1682.2030. Accessed: Jul. 1, 2023. [Online]. Available: https://www.degruyter.com/document/doi/10.2202/1935-1682.2030/html .

[16] P. R. Brown and F. M. O'Sullivan, "Spatial and temporal variation in the value of solar power across United States electricity markets," en, *Renewable and Sustainable Energy Reviews*, vol. 121, p. 109 594, Apr. 2020, ISSN: 1364-0321. DOI: 10.1016/j.rser.2019.109594. Accessed: Jul. 1, 2023. [Online]. Available: https://www.sciencedirect.com/science/article/pii/S1364032119308020 .

[17] M. Vanatta, M. T. Craig, B. Rathod, J. Florez, I. Bromley-Dulfano, and D. Smith, "The costs of replacing coal plant jobs with local instead of distant wind and solar jobs across the United States," en, *iScience*, vol. 25, no. 8, p. 104 817, Aug. 2022, ISSN: 25890042. DOI: 10.1016/j.isci.2022.104817. Accessed: Jul. 1, 2023. [Online]. Available: https://linkinghub.elsevier.com/retrieve/pii/S2589004222010896 .

[18] M. Carrión and R. Zárate-Miñano, "Operation of renewable-dominated power systems with a significant penetration of plug-in electric vehicles," en, *Energy*, vol. 90, pp. 827–835, Oct. 2015, ISSN: 0360-5442. DOI: 10.1016/j.energy.2015.07.111. Accessed: Jun. 25, 2023. [Online]. Available: https://www.sciencedirect.com/science/article/pii/S0360544215010063 .

[19] A. Jenn, K. Clark-Sutton, M. Gallaher, and J. Petrusa, "Environmental impacts of extreme fast charging," en, *Environmental Research Letters*, vol. 15, no. 9, p. 094 060, Aug. 2020, Publisher: IOP Publishing, ISSN: 1748-9326. DOI: 10.1088/1748-9326/ab9870. Accessed: Apr. 29, 2024. [Online]. Available: https://dx.doi.org/10.1088/1748-9326/ab9870 .

[20] A. Weis, J. J. Michalek, P. Jaramillo, and R. Lueken, "Emissions and Cost Implications of Controlled Electric Vehicle Charging in the U.S. PJM Interconnection," en, *Environmental Science & Technology*, vol. 49, no. 9, pp. 5813–5819, May 2015, ISSN: 0013-936X, 1520-5851. DOI: 10.1021/es505822f. Accessed: Oct. 6, 2020. [Online]. Available: https://pubs.acs.org/doi/10.1021/es505822f .

[21] P. Nunes and M. C. Brito, "Displacing natural gas with electric vehicles for grid stabilization," en, *Energy*, vol. 141, pp. 87–96, Dec. 2017, ISSN: 0360-5442. DOI: 10.1016/j.energy.2017.09.064. Accessed: Jul. 1, 2023. [Online]. Available: https://www.sciencedirect.com/science/article/pii/S0360544217315852 .

[22] K. E. Forrest, B. Tarroja, L. Zhang, B. Shaffer, and S. Samuelsen, "Charging a renewable future: The impact of electric vehicle charging intelligence on energy storage requirements to meet renewable portfolio standards," en, *Journal of Power Sources*, vol. 336, pp. 63–74, Dec. 2016, ISSN: 0378-7753. DOI: 10.1016/j.jpowsour.2016.10.048. Accessed: Jun. 25, 2023. [Online]. Available: https://www.sciencedirect.com/science/article/pii/S0378775316314409 .

[23] B. Tarroja, L. Zhang, V. Wifvat, B. Shaffer, and S. Samuelsen, "Assessing the stationary energy storage equivalency of vehicle-to-grid charging battery electric vehicles," *Energy*, vol. 106, pp. 673–690, Jul. 2016, ISSN: 0360-5442. DOI: 10.1016/j.energy.2016.03.094. Accessed: Aug. 13, 2025. [Online]. Available: https://www.sciencedirect.com/science/article/pii/S0360544216303383 .

[24] PJM, "Energy Transition in PJM: Frameworks for Analysis," Tech. Rep., Dec. 2021. [Online]. Available: https://pjm.com/-/media/committees-groups/committees/mrc/2021/20211215/20211215-item-09-energy-transition-in-pjm-whitepaper.ashx .

[25] L. Vimmerstedt, T. Stehly, S. Akar, A. Sekar, B. Mirletz, D. Stright, C. Augustine, P. Beiter, P. Bhaskar, N. Blair, S. Cohen, W. Cole, P. Duffy, D. Feldman, P. Gagnon, P. Kurup, C. Murphy, V. Ramasamy, J. Robins, J. Zuboy, D. Oladosu, and J. Hoffmann, "2022 Annual Technology Baseline (ATB) Cost and Performance Data for Electricity Generation Technologies," English, DOE Open Energy Data Initiative (OEDI); National Renewable Energy Laboratory (NREL), Tech. Rep. 5716, Jun. 2022. DOI: 10.25984/1871952. Accessed: Jul. 23, 2023. [Online]. Available: https://www.osti.gov/dataexplorer/biblio/dataset/1871952 .

[26] R. Lueken and J. Apt, "The effects of bulk electricity storage on the PJM market," en, *Energy Systems*, vol. 5, no. 4, pp. 677–704, Dec. 2014, ISSN: 1868-3975. DOI: 10.1007/s12667-014-0123-7. Accessed: Jul. 20, 2023. [Online]. Available: https://doi.org/10.1007/s12667-014-0123-7 .

[27] M. Bruchon, Z. L. Chen, and J. Michalek, "Cleaning up while Changing Gears: The Role of Battery Design, Fossil Fuel Power Plants, and Vehicle Policy for Reducing Emissions in the Transition to Electric Vehicles," *Environmental Science & Technology*, vol. 58, no. 8, pp. 3787–3799, Feb. 2024, ISSN: 0013-936X. DOI: 10.1021/acs.est.3c07098. Accessed: May 8, 2024. [Online]. Available: https://doi.org/10.1021/acs.est.3c07098 .

[28] A. Weis, P. Jaramillo, and J. Michalek, "Consequential life cycle air emissions externalities for plug-in electric vehicles in the PJM interconnection," en, *Environmental Research Letters*, vol. 11, no. 2, p. 024 009, Feb. 2016, Publisher: IOP Publishing, ISSN: 1748-9326. DOI: 10.1088/1748-9326/11/2/024009. Accessed: Apr. 25, 2024. [Online]. Available: https://dx.doi.org/10.1088/1748-9326/11/2/024009 .

[29] B. Sergi and W. Cole, "Operating Reserves in ReEDS," English, National Renewable Energy Lab. (NREL), Golden, CO (United States), Tech. Rep. NREL/PR-6A40-81706, Dec. 2021. DOI: 10.2172/1841961. Accessed: Jul. 26, 2023. [Online]. Available: https://www.osti.gov/biblio/1841961 .

[30] M. T. Craig, P. Jaramillo, H. Zhai, and K. Klima, "The Economic Merits of Flexible Carbon Capture and Sequestration as a Compliance Strategy with the Clean Power Plan," *Environmental Science & Technology*, vol. 51, no. 3, pp. 1102–1109, Feb. 2017, Publisher: American Chemical Society, ISSN: 0013-936X. DOI: 10.1021/acs.est.6b03652. Accessed: Jul. 26, 2023. [Online]. Available: https://doi.org/10.1021/acs.est.6b03652 .

[31] "EPA Report on the Social Cost of Greenhouse Gases: Estimates Incorporating Recent Scientific Advances," Tech. Rep., Nov. 2023.